universität wien

MASTERARBEIT

Quantification of fold growth (Permam-, Bana Bawi- and Safeen Anticlines, NE Iraq)

Bernhard Bretis, Bakk.rer.nat.

gemeinsam mit

Nikolaus Bartl, Bakk.rer.nat.

Zur Erlangung des akademischen Grades

Master of Science (MSc.)

Wien, 2010

Studienkennzahl lt. Studienblatt:	A 066 815
Studienrichtung lt. Studienblatt:	Masterstudium Erdwissenschaften UG2002
Betreuerin / Betreuer:	Univ.Prof.Mag.Dr. Bernhard Grasemann

"With their four-dimensional minds,
and in their interdisciplinary ultra verbal way,
geologists can wiggle out of almost anything."
-John McPhee

"I haven't failed, I've found 10,000 ways that don't work"
-Thomas Alva Edison

Motivation und Begründung zur gemeinsamen Verfassung der Masterarbeit

Die einzigartige Möglichkeit, im Rahmen eines von der OMV subventionierten Projektes, thematisch neue Methoden in einem bisher kaum zugänglichen und deshalb auch sehr wenig bearbeiteten Teil des geologisch hochinteressanten Zagrosgebirges für die Verfassung unserer Masterarbeiten anzuwenden, begeisterte uns (Nikolaus Bartl und Bernhard Bretis) von Anfang an.

Aus politischen und kulturellen Gründen ergeben sich in einem Land wie dem Irak spezielle Anforderungen an die Organisation und Durchführung einer Geländearbeit. Es war daher klar, daß aus sicherheitstechnischen und organisatorischen Gründen nur ein gemeinsamer Geländeaufenthalt Sinn machen würde. So konnten wir beide uns mit der jeweiligen Unterstützung des anderen auf unsere Gebiete fokussieren.

Durch die geologisch und methodisch unmittelbare Verwandheit unserer Themen, sowie die Absicht der Veröffentlichung in komprimierter und wissenschaftlich fundierter Form in einem der Thematik entsprechenden Journal, kamen wir zu dem Entschluss, dass nur eine gemeinsame Verfassung unserer Masterarbeiten (gemäß studienrechtlichem Teil der Satzung der Universität Wien §15 Abs. 6), der Komplexität des Themas gerecht werden kann. Die Verschmelzung zu einem gemeinsamen Ganzen erfolgte sukkzessive während der Ausarbeitung der einzelnen Themenbereiche.

Thematisch erfolgte die Aufteilung der Bearbeitungsgebiete geographisch, wobei sich Nikolaus Bartl auf die Safeen Antiklinale und Bernhard Bretis auf die Permam-Bana Bawi Antiklinalen konzentrierte.

Acknowledgements

First, I want to thank my supervisor Bernhard Grasemann for the great opportunity to work on this master thesis. Especially his support and patience in various discussions as well as his enthusiasm for solving geological questions is appreciated.

Special thanks to the OMV who supported this master thesis financially and made it possible to realize a safe and well organized field trip to NE Iraq. I want to thank Gerhard Milan, Duncan Lockhart, Dana Mawlood, Azad Ibrahim for the organization but especially Sheriff, Aram and all the other Iraqis, who supported us in field and made our trip very entertaining.

Many thanks to my colleague Nikolaus Bartl for the excellent collaboration during the time we worked on this master thesis where we spent lots of time holding countless sometimes more, sometimes less useful, interesting and productive discussions and for the enjoyable time during our study.

Daniel Reif I want to thank for his support in the field and whenever else it was needed.

Erich Draganits for helping us to solve geomorphologic questions and Robert Faber for his support in remote sensing issues.

My university mates Magda Bottig, Christine Dunkel, Vanessa Fremd, Richi Laner, Jürgen "Yrga" Leitner, Linda Lerchbaumer, Clemens Porpazcy, Alex Rath, Hans Reitinger, Andrea Schicker, Christian "Schrotti" Schrott, Johannes Steinbrener, Jonas Weil and Helga Zeitlhofer I would like to thank for the many amusing hours we spent together in university, on numerous excursions and various events. Because of all of you the years of study, especially the countless adventurous excursions will stay unforgettable!
Special thanks to Christian "Schrotti" Schrott for being a sober and commodious roommate on various excursions and journeys and to Jürgen "Yrga" Leitner for his almost daily coffee service.

Last but not least a big "thank you" to my family, especially my parents, who not only enabled me to study financially but also always supported me in words and deeds whenever it was needed.

Abstract (Bartl/Bretis)

The Zagros Mountains extend over 1800 km from Kurdistan in N-Iraq to the Strait of Hormuz in Iran and is one of the world most promising regions for the future hydrocarbon exploration. The orogen started to form as a result of the collision between the Eurasian and Arabian Plates, whose convergence began in the Late Cretaceous as part of the Alpine–Himalayan orogenic system. Geodetic and seismological data document that both plates are still converging and that the fold and thrust belt of the Zagros is actively growing.

Recent kinematic models based on GPS networks suggest a north-south shortening between Arabian and Eurasian in the order of 1.5-2.5 cm/yr.

Extensive hydrocarbon exploration mainly focuses on the antiforms of this fold and thrust belt and therefore the growth history of the folds is of great importance.

The Zagros fold and thrust belt is of great economic interest because it has been estimated that this area contains about 15% of the global recoverable hydrocarbons. Whereas the SE parts of the Zagros have been investigated by detailed geological studies, the NW extent being part of the Republic of Iraq have experienced considerably less attention.

In this master thesis we combine field work and remote sensing techniques in order to investigate the interaction of erosion and fold growth in the area NE of Erbil (Kurdistan, Iraq). This part of the Zagros fold and thrust belt belongs to the so-called Simply Folded Belt, where faults or fault related folds have only minor importance. The mechanical anisotropy of the formations consisting of a succession of relatively competent (massive dolomite and limestone) and incompetent (claystone and siltstone) sediments essentially controls the deformation pattern with open to gentle parallel folding of the competent layers and flexural flow folding of the incompetent layers.

In particular we focus on the interaction of the transient development of drainage patterns along growing antiforms, which directly reflects the kinematics of progressive fold growth.

Using an ASTER digital elevation model in combination with geological field data we quantified 250 drainage basins along the different limbs of the subcylindrical Permam, Bana Bawi- and Safeen- Anticlines. Geomorphological indices of the drainage basins (spacing and elongation ratio, circularity index and shape factor) of different parts in the fore and back-limb of the anticlines demonstrate that the basins have a low maturity and that fold growth is still highly active.

These folds have been detected by mapping ancient and modern river courses that initially cut the nose of growing folds and eventually got defeated leaving behind a wind gap. Wind gaps

are probably the best indicator for lateral fold growth directions, and are therefore used extensively in this thesis.

Fold segments, propagating in different directions force rivers to join resulting in steep gorges, which dissect the merging fold noses. Along rapidly lateral growing folds (e.g. at the SE end of the Bana Bawi Anticline) we observed “curved wind gaps”, a new type of abandoned river course, where the form of the wind gap mimics a formed nose of a growing antiform. The inherited curved segments of uplifted curved river courses strongly influence the development of the drainage system. This new model helps to detect embryonic fold segments of subcylindrical folds, which are otherwise difficult to identify.

Most importantly, the results of these geomorphological investigations clearly demonstrate that the subcylindrical folds have developed from several non-cylindrical embryonic folds, which have merged during progressive fold growth.

Zusammenfassung (Bartl/Bretis)

Das Zagros Gebirge erstreckt sich über 1800 km von Kurdistan im Nordirak bis zur Straße von Hormuz im Iran und ist eine der vielverprechendsten Regionen für zukünftige Kohlenwasserstoffexploration.
Das Zagros Orogen resultiert aus der Kollision der eurasischen mit der arabischen Platte, deren Konvergenz in der Oberkreide als ein Teil der Alpidischen Orogenese begann. Geodätische und seismologische Daten dokumentieren eine rezente Konvergenz der beiden Platten und ein anhaltendes Wachstum des Falten- und Überschiebungsgürtels des Zagros. Neue, GPS - basierte kinematische Modelle gehen von einer Nord-Süd-Verkürzung von 1.5 – 2.5 cm/a zwischen der eurasischen und der arabischen Platte aus.
Die Kohlenwasserstoffexploration konzentriert sich hauptsächlich auf die Antiformen dieses Falten und Überschiebungsgürtels, wobei die Wachstumsgeschichte der Falten von übergeordneter Bedeutung ist.
Der Falten- und Überschiebungsgürtel des Zagros ist von großem wirtschaftlichen Interesse, da diese Region 15% der weltweit förderbaren Kohlenwasserstoffreserveren beherbergt. Während der südöstliche Abschnitt des Zagros durch diverse geologische Untersuchungen bereits intensiv bearbeitet wurde, erfuhr der nordöstliche, irakische Teil viel weniger Aufmerksamkeit.
In dieser Masterarbeit verbinden wir Geländearbeit mit Fernerkundungstechniken um das Zusammenspiel von Erosion und Faltenwachstum in der Region nordöstlich von Erbil (Kurdistan, Irak) zu untersuchen.
Dieser Abschnitt des Zagros ist Teil des sogenannten „simply folded belt“, in dem Störungen und störungsgebundene Falten nur untergeordnet von Bedeutung sind.
Die Kompetenzkontraste zwischen relativ kompetenten (massiver Dolomit und Kalk) und inkompetenten Sedimenten (Silt unnd Tonstein) kontrollieren die Deformationsmechanismen mit einer hohen bis mittleren Faltungswellenlänge der kompetenten Schichten und „flexural flow folding“ der inkompetenten Schichten.
Der Fokus liegt auf der Interaktion zwischen Geomorphologie und Tektonik, die die Kinematik und das fortschreitende Wachstum der Falten reflektiert.
Zur Quantifizierung von 250 Entwässerungsgebieten entlang der Permam, Bana Bawi- und Safeen- Antiklinalen wurde ein digitales Höhenmodell (ASTER) in Kombination mit den im Feld gewonnenen Daten herangezogen.

Vier verschiedene geomorpholgische Indizes (Spacing Ratio, Elongation Ratio, Circularity Index und Shape Factor) wurden entlang der Forelimbs und der Backlimbs der Antiklinalen berechnet und führen zu der Annahme einer niedrigen Maturität und einer immer noch hohen Wachstumsrate der Falten.
Auf diesen Falten wurden ehemalige und rezente Flussläufe kartiert, die zuerst in die Nase der wachsenden Falten einschnitten und später von den wachsenden Antiformen abgelenkt wurden, was zur daraus resultiernden Enstehung von Wind Gaps führte. Diese Wind Gaps stellen den wohl besten Hinweis für laterale Faltenwachstumsrichtungen dar und werden daher intensiv in dieser Arbeit analysiert.
In verschiedene Richtungen wachsende Faltensegmente führen zu einer Ablenkung beziehungsweise in weiterer Folge zu einem Zusammenmünden von Flüssen und zur Entstehung von steilen Schluchten zwischen den zusammenwachsenden Falten.
Enlang von sehr schnell wachsenden Falten (z.B. am südöstlichen Ende der Bana Bawi Antiklinale), wurde ein neues geomorpholgisches Kriterium – „Curved Wind Gaps“ – definiert. Bei diesem neuen Typus von abgelenkten Flussläufen zeichnet die Form des Wind Gaps die Form der Faltennase nach. Diese „Curved Wind Gaps“ haben in weiterer Folge einen großen Einfluss auf das neu entstehende Entwässerungsnetz.
Dieses neue Modell ist bei der Erkennung von embrionischen Faltensegmenten von subzylindrischen Falten, die ansonsten schwer identifizierbar sind, hilfreich.
Diese geomorphologischen Beobachtungen führen zu der wichtigen Erkenntnis, dass die subzylindrischen Falten aus mehreren nicht- zylindrischen embrionischen Falten, die sich während des Wachstums vereinten, zusammengesetzt sind.

Contents

Motivation und Begründung zur gemeinsamen Verfassung der Masterarbeit V

Acknowledgements VII

Abstracts IX

Abstract (Bartl/Bretis)

Zusammenfassung (Bartl/Bretis)

1. Introduction (Bartl/Bretis) 3

2. Geological overview 5

2.1. Regional tectonics (Bretis) 5

2.2. Lithology and stratigraphy (Bartl) 7

3. Methodology (Bartl/Bretis) 13

3.1. Geomorphology (Bartl/Bretis) 13

3.2. Development of wind gaps and asymmetric tributary networks during lateral propagation of folds (Bartl) 14

3.3. New process: Curved wind gaps (Bretis) 16

3.4. Development of hogbacks drawn on the example of Bana Bawi Anticline (Bretis) 18

3.5. Quantification of geomorphologic parameters (Bartl/Bretis) 19

4. Results 23

4.1. Geomorphologic criteria and growth quantification (Bartl/Bretis) 23

4.1.1. Bana Bawi and Permam anticlines (Bretis) 26

4.1.1.1. Bana Bawi Anticline 26

4.1.1.2. Permam Anticline 29

4.1.2. Safeen Anticline (Bartl) 30

4.2. Quantification of geomorphologic parameters (Bartl/Bretis) 33

5. Conclusion (Bartl/Bretis) 37

6. References 39

7. Appendix (all data are separated into data processed by Bernhard Bretis (Permam-, Bana Bawi Anticlines) and Nikolaus Bartl (Safeen Anticlines)) 45

7.1. Abbreviations 45

7.2. Overview of the statistics (Bartl/Bretis) 47

7.3. Detailed statistics 50

7.3.1. Fold segments of Permam-, Bana Bawi Anticlines (Bretis) 50

7.3.2. Fold segments of Safeen Anticline (Bartl) 65

7.4. List of figures 77

8. Curriculum Vitae 79

1. Introduction (Bartl/Bretis)

The interaction of erosion and tectonics in fold and thrust belts is of major interest in recent literature, because they are estimated to contain 14% of the known and 15% of the undiscovered global recoverable hydrocarbons. Especially the Zagros, containing 49% of global fold and thrust belt related hydrocarbons, is of great importance [Ries, Butler, Graham and references cited there, 2007].

Geomorphology is an excellent tool to draw conclusions about the tectonic evolution and fold growth [i.e. Jackson et al, 1996; Burbank et al, 1999; Burbank & Pinter, 1999; Keller et al, 1999; Burbank & Anderson, 2001; Delcaillau, 2001; Delcaillau et al 2006; Tsodoulos et al, 2008]. The results of studies like this are a very important feature in hydrocarbon industry to understand the structure and usability of potential hydrocarbon reservoirs.

Relationships between active tectonics and erosional landforms reveal differences in the type and rates of deformation and fold growth [Delcaillau et al 2006].

The evolution and changes in drainage patterns as well as the influence of fold growth to their appearance are evidence for the kinematics of folds and faults [Jackson et al, 1998].

Tributary networks act very sensitive to tectonics and so generate characteristic geomorphologic shapes that can be used for the interpretation of tectonic processes [Burbank & Anderson, 2001].

Due to a broad offer and good availability of digital elevation models and aerial photographs this method offers great applicabilities which caused the development of various new interpretation methods in the last few years [i.e. Davis et al, 2003; Davis et al, 2005; Burberry et al, 2008; Hilley & Arrowsmith, 2008; Ramsey et al, 2008].

Numerical modelling of folding versus faulting in convergent continental settings offer new possibilities in the way of understanding the kinematics of fold and thrust belts [Simpson, 2006; Simpson, 2009]. I.e. Simpson, 2006, shows mathematical models of the interactions between fold and thrust belt deformation, foreland flexure and surface mass transport/erosion.

The major goal of this paper is to use geomorphologic criteria to develop a detailed evolution model of Bana Bawi, Permam and Safeen anticlines. These anticlines are situated in an area of about 1000 km² northeast of the city of Erbil (NE Iraq), which is considered to be a major oil target in the future and is very suitable for the use of geomorphology to quantify fold evolution. We first briefly discuss the regional tectonic settings and the stratigraphy of the

investigation area. Furthermore we describe the most important geomorphologic criteria and parameters used in this study as well as their application on the earlier described anticlines.

2. Geological Overview

2.1. Regional tectonics (Bretis)

The Zagros Fold and Thrust Belt is a seismically active orogen, which extends over 1800 km from Northern Iraq to the Strait of Hormuz in Iran. The Zagros Mountains started to form as a result of the collision between the Eurasian and Arabian Plates, whose convergence began in the Late Cretaceous and was the last of a series of extensional–convergent events within the extensive Alpine–Himalayan orogenic system [Dewey et al, 1973; Dercourt et al, 1986]. Recent measurements between the two tectonic plates have identified a rate of collision of approximately 1.6 – 2.2 cm/yr [Sella et al, 2002] in the last 10 Ma which is assumed as the minimum age of continental collision [McQuarrie et al, 2003] (Fig. 1). Triassic and Jurassic were dominated by alternating rifting events and passive continental margin phases in the northeastern part of the present-day Arabian Peninsula. Late Titonian to Cenomanian was characterized by opening of the southern Neo-Tethyan Ocean, where seafloor-spreading took place in northeastern direction. From Turonian to Eocene the Neo-Tethys was closing and a foreland basin formed around the margin of the Arabian Plate.

Continent-continent collision started in Oligocene and is active until present day. [Jassim & Goff, 2006]

The deformation in the simply folded belt started between 8 Ma [Homke et al, 2004] and 5 Ma [Allen et al, 2002].

Most of this deformation is partitioned within the Zagros Mountains in south-southwest oriented folding and thrusting with northwest-southeast to north-south trending dextral strike slip faults.

Whereas the tectonic structure and the geomorphological response to active deformation are thoroughly studied in the southern part of the Zagros in Iran, there are almost no modern field based studies of the Zagros in Northern Iraq.

From northeast to southwest the Zagros belt comprises four units, all of which got their individual characteristics and deformation style:

(1) the Sanandaj-Sirjan metamorphic zone (2) the thrust dominated Imbricated Zone (3) the Simply Folded Belt, (4) the Mesopotamian foreland basin with buried folds, which extends to the Persian Gulf in southeastern direction [Homke et al, 2004].

The Main Zagros Thrust borders the Imbricated Zone towards the northeast and is proposed to be the suture zone between Eurasian and Arabian plates [Dewey et al, 1973; Dercourt et al, 1986]. The fault is characterised by thrusting as well as by a dextral strike-slip displacement. The Imbricated Zone, which contains highly imbricated slices of the sedimentary cover as well as fragments of cretaceous ophiolites [Berberian, 1995], is up to 25 km wide [Jassim & Goff, 2006] and is bordered towards southwest by the northwest-southeast trending High Zagros Fault [Berberian, 1995] which divides it from the Simply Folded Belt. This thrust mainly does not cut through to the surface. Cretaceous and older units in this zone are transversed by reverse faults dislocating the anticlines into imbricates, which means that the anticlines often over-ride the synclines [Jassim & Goff, 2006]. The Mountain Front Fault which coincides over 3000 m of displacement [Jassim & Goff, 2006], is the southwestern boundary of the simply folded belt [Berberian, 1995], which has a width between 25 and 50 km [Jassim & Goff, 2006]. The folds in this area, mostly with broad box like geometry, are separated by narrow synclines. The structures are mainly asymmetrical with steep SW to S flanks along with reverse faults [Jassim & Goff, 2006] (Fig. 1).

The investigation area as part of the simply folded belt is situated northeast of Erbil (NE Iraq) (Fig. 1). Shortening in the simply folded belt comprises thin- and thick- skinned deformation [Mouthereau et al, 2007; Oveisi et al, 2009]. The investigation area however shows classic thin- skinned deformation. Surface faults are widely absent in this region. The sedimentary cover in the iraqian part of the simply folded belt is about 9-10 km thick [Jassim & Goff, 2006]. By folding these thick multilayered sequences space problems in the core of the fold occur. Because of the broad absence of large evaporite horizons (like the Hormuz salts in Iran) in northeastern Iraq, it is very likely that this space problem is solved by movement of other soft sediments like shales. This leads to amplitude and wavelength differences between sediment layers within the fold.

The fold wavelengths in the Imbricated Zone of northeastern Iraq averages between 4 and 10 km, which is much less than an average between 15 and 25 km of those in Iran with a maximum up to 35 km as described by Mouthereau et al, 2007.

The shape of the folds in the simply folded belt is mainly sub-cylindrical with wavelengths between about 6 and 10 km, which again is less than in Iran, where it averages between 10 and 20 km.

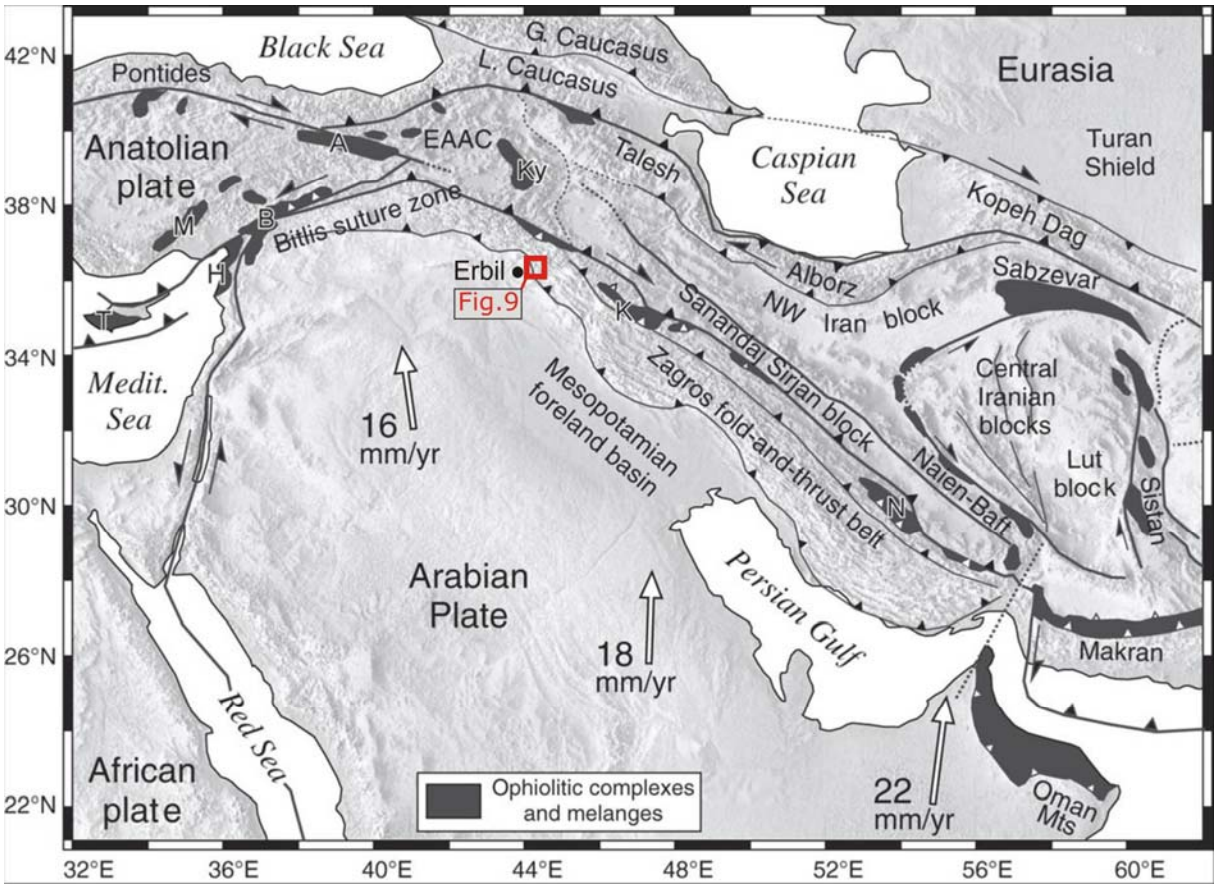

Figure 1: Regional tectonic setting of the Zagros Mountains. MFF (Mountain Front Fault), HZF (High Zagros Fault), MZT (Main Zagros Thrust); the red rectangle shows the investigation area. Velocities of movement from Sella et al, 2002; Modified after Homke et al, 2009;

2.2. Lithology and stratigraphy (Bartl)

The oldest sediments outcropping in northeastern Iraq are Triassic shales, black limestone and dolomites of the Baluti and Kurra Chine Formation. Together the total thickness of these two Formations is up to 1200 m.

Lower Jurassic Sehkaniyan and Sarki Formations were deposited in restricted lagoons and combined they are about 600 m thick. They mainly consist of thin bedded limestone, dolomites and shales.

Middle to upper Jurassic Chia Gara (30 – 300 m thick), Barsarin (20 m thick), Naokelekan (20 m thick) and Sargelu (115 m thick) Formations comprise mainly bedded to massive dolomites, limestone and marl.

The Lowest Cretaceous is represented by Balambo (up to 900 m thick), Garagu (200 m thick) and Sarmord (600 m thick) Formations built up mainly by limestone, dolomites and marls.
The oldest sediments outcropping in the investigation area are part of the Qamchuqa Formation which represents a clastic-carbonate ridge of Hauterivian to Albian age. Mainly it is built up by thick bedded detrital, organodetrital and argillaceous limestone with variable degrees of dolomitisation and an average thickness up to 500 m.
The Campanian to Maastrichtian Aqra – Bekhme Formation unconformably overlies the Qamchuqa Formation with a thickness of about 300 to 500 m. It is defined as a reef limestone complex with massive rudists, shoal facies and detrital forereef limestone and a basal breccia conglomerate. It is locally dolomitised, siliceous and impregnated with bitumen.
The next stratigraphic unit is the Shiranish Formation of same age, which was deposited in an outer shelf basin. It comprises thin bedded argillaceous limestone overlain by blue pelagic marls with a total formation thickness of about 400 m.
Next to the carbonate ramp a rapidly subsiding foredeep basin established simultaneously in front of the naps of the obducted margin of the southern Neo-Tethys. The typical flysch sediments of the Tanjero Formation where deposited in this basin: pelagic marl, argillaceous limestone beds and siltstone beds in the lower part; and silty marl, sandstone, conglomerates and sandy or silty organo-detrital limestone (thickness: varies from a few meters up to 2000 m)
The Campanian to Maastrichtian deposits are followed by Selandian to Thanetian Kolosh Formation with an average thickness of 400 m. The depositional environment is a marginal marine, rapidly subsiding trough. The sediments of this formation are mainly mudstones, siltstones and argillaceous limestone.
The calcareous beds of the Khurmala Formation interfinger with the clastic sediments of the Kolosh Formation due to a probable connection of its depositional basin to the Kolosh trough. The thickness of the Khurmala Formation is about 185 m.
The about 210 m thick, Lutetian to Bartonian Avanah Formation comprises mainly dolomitised and recrystallized limestone with a probable unconformity in the lower contact. The depositional environment was an isolated carbonated shoal associated with a palaeoridge along the northeast shoreline of the basin during a sea level high. North and northeast of this barrier the molasse basin of the Ypresian to Lutetian Gercus Formation was situated. This formation comprises up to 850 m massive red and purple shales, mudstones, sandy marls, pebbly sandstones and conglomerates.

The Bartonian to Priabonian Pila Spi Formation, lying on top of interfingering Gercus and Avanah Formations, is between 100 and 200 m thick and built up by well bedded, white, bituminous, chalky and crystalline limestone containing chert nodules. It was deposited in a shallow lagoon.

The following stratum is the Fatha (Lower Fars) Formation (Burdigalian to Serravallian) that comprises anhydrite, gypsum and salt interbedded with limestone, mudstone and marl, up to 900 m thick. In our investigation area especially mudstones, marls and other clastics dominated. It was deposited in a rapidly subsiding basin which periodically became evaporitic.

Injana (Upper Fars) Formation (Tortonian to Messinian) contains fine grained pre-molasse sediments, deposited initially in costal areas and later in a fluviolacustrine system, with a thickness of up to 900m. Northeast of Erbil these are mainly sands deriving from the rising Zagros Mountains.

The youngest Tertiary sediments are part of Bakhtiari Formation which has to be divided into Mukdadiya (Lower Bakhtiari) and Bai Hassan (Upper Bakhtiari) Formations. The Mukdadiya Formation comprise up to 2000 m of fining upwards cycles of gravely sandstone, sandstone and red mudstone deposited in a fluvial environment of a rapidly subsiding foredeep basin whereas Bai Hassan Formation mostly consists of a conglomeratic facies originating of alluvial fans in the foreland of the High Folded Zone that can be up to 3000 m thick. (Fig. 2) [Jassim & Goff and references cited there, 2006]

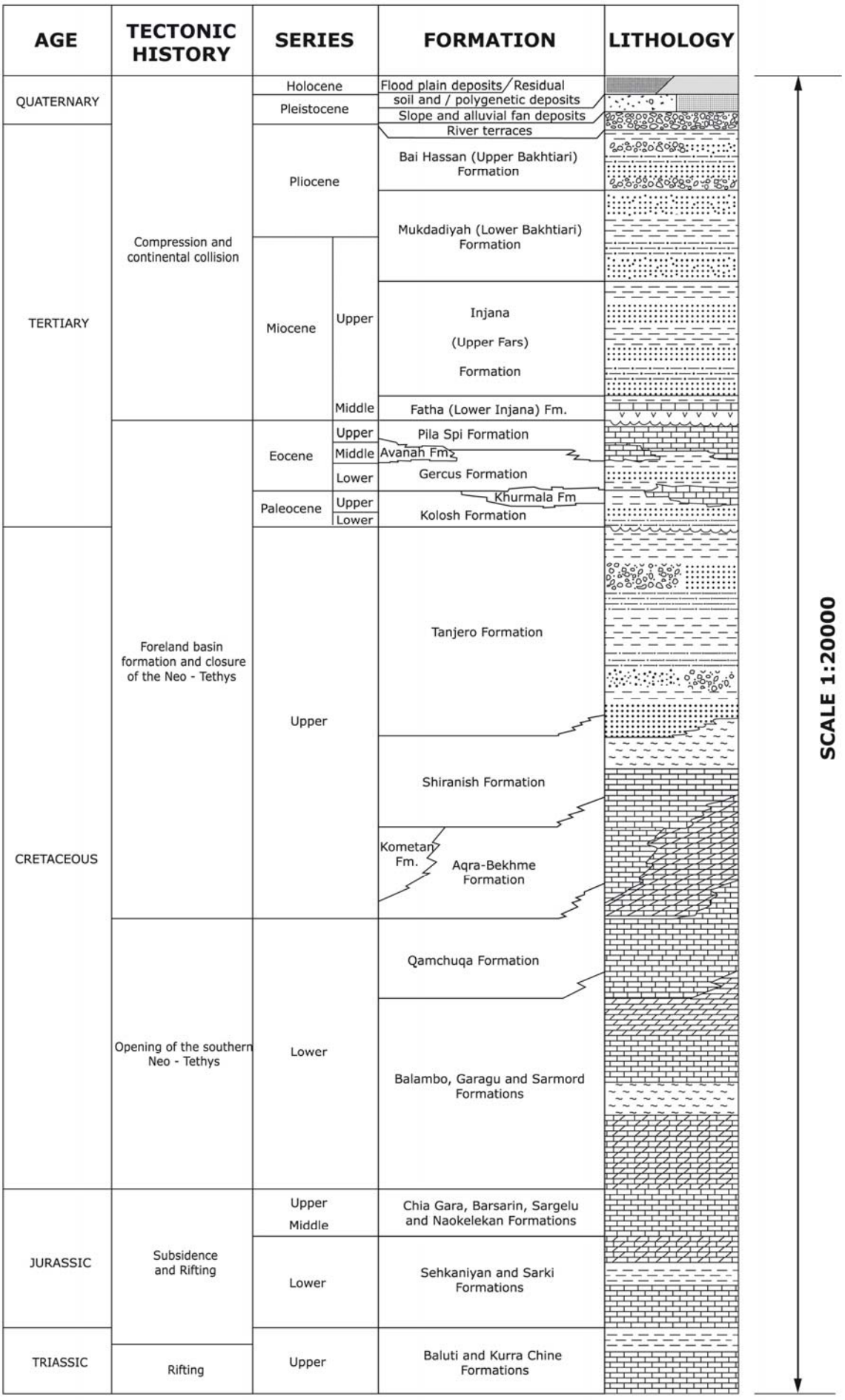
AGE
TECTONIC HISTORY
SERIES
FORMATION
LITHOLOGY
QUATERNARY
TERTIARY
CRETACEOUS
JURASSIC
TRIASSIC
Holocene
Pleistocene
Pliocene
Miocene
Upper
Middle
Eocene
Upper
Middle
Lower
Paleocene
Upper
Lower
Upper
Lower
Upper
Middle
Lower
Upper
Compression and continental collision
Foreland basin formation and closure of the Neo - Tethys
Opening of the southern Neo - Tethys
Subsidence and Rifting
Rifting
Flood plain deposits / Residual soil and / polygenetic deposits
Slope and alluvial fan deposits
River terraces
Bai Hassan (Upper Bakhtiari) Formation
Mukdadiyah (Lower Bakhtiari) Formation
Injana (Upper Fars) Formation
Fatha (Lower Injana) Fm.
Pila Spi Formation
Avanah Fm.
Gercus Formation
Khurmala Fm
Kolosh Formation
Tanjero Formation
Shiranish Formation
Kometan Fm.
Aqra-Bekhme Formation
Qamchuqa Formation
Balambo, Garagu and Sarmord Formations
Chia Gara, Barsarin, Sargelu and Naokelekan Formations
Sehkaniyan and Sarki Formations
Baluti and Kurra Chine Formations
SCALE 1:20000

Figure 2: Major stratigraphic units and tectonic events of the Zagros in northeastern Iraq (modified after Sattarzadeh et al, 2002); Lithology digitized from the geological map of Arbeel and Mahabad Quadrangles (Sissakian, 1997)

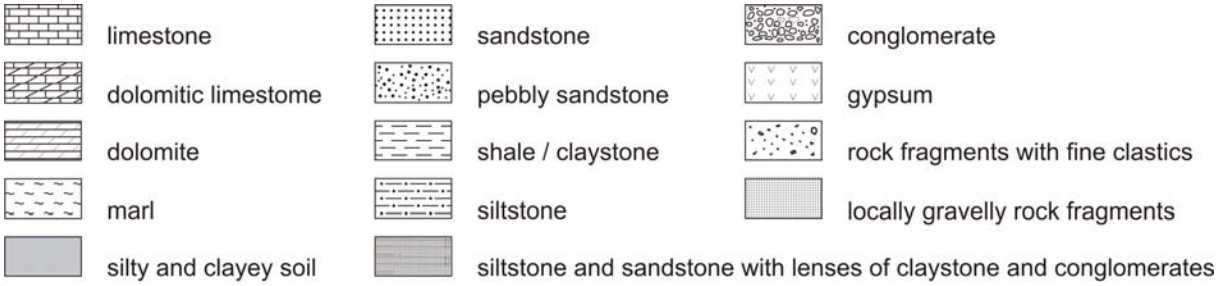

Figure 3: Legend for the lithologic symbols used in Figure 2.

Differences in structure and composition of these lithologies resulting in a changing weathering resistivity and landscape are some of the reasons that allow the use of geomorphological methods described in the following to quantify fold growth.

3. Methodology (Bartl/Bretis)

The remote sensing investigations are based on a 30m ASTER DEM combined with false color composite satellite images consisting of 4 spectral bands.
Digital stream networks were generated from this DEM using the “Imposed gradients plus” method, which is an extension of the “Imposed gradients” method proposed by Garbrecht and Martz (1997), within Rivertools 3.0. This method refines flow within flats to achieve the aim to virtually eliminate all parallel flow. The river network was then categorized using the Strahler system [Strahler, 1964].
Furthermore the catchment areas of the rivers on the limbs of the anticlines were extracted and then analyzed concerning their scales.
Geomorphologic parameters, such as sinuosity, slope, spacing ratio, elongation ratio, circularity index and basin shape were calculated for various areas to quantify the obvious differences in various parts of the anticlines [Talling, 1997]. Variations in the habit of the generated tributary patterns were one of the criteria used to recognize fold growth directions. The different drainage patterns as well as profiles perpendicular to the fold axis, generated from DEM, were used to determine a relative age sequence.

3.1. Geomorphology (Bartl/Bretis)

Geomorphology is an excellent instrument to categorize the direction of lateral fold propagation. If folds are propagating, complex river patterns and topography can sometimes reveal the history of lateral propagation and vertical growth [Burbank & Anderson, 2001]. Keller et al. (1999) describe six main geomorphic criteria to evaluate these rates: (a) the decrease of drainage density and degree of dissection of the landscape on the fold crest in direction of fold propagation; (b) the decrease in rotation and inclination of the forelimb; (c) the decrease in relief of a topographic profile along the fold crest; (d) the deformation of progressively younger deposits or landforms; (e) the development of characteristic drainage patterns; (f) the occurrence of series of wind gaps with decreasing elevation in propagation direction. The last three of these criteria are considered to be the strongest indicators for lateral fold propagation [Keller et al, 1999; Ramsey et al, 2008].

Especially the presence of a series of wind gaps is intuitively to identify and represents the most powerful indicator to determine lateral propagation directions.
Drainage patterns are very sensitive to changes in the surface slope and therefore record fold growth and evolution excellently [Jackson et al, 1996]. This sensitivity to changes in fold geomorphology leads to the development of distinctive asymmetric forked tributary patterns showing the direction of fold propagation.
Due to the importance of these two criteria for these studies they will be discussed in detail in the following sections.
Furthermore great differences in the strata cause the recent appearance of the area. More competent layers show stronger resistivity to erosion and hence form hogbacks. Hogbacks can be described as homoclinal ridges that form due to lithological contrasts and different weathering rates.

3.2. Development of wind gaps and asymmetric tributary networks during lateral propagation of folds (Bartl)

Two of the most undisputed and powerful tools in tectonic geomorphology used for the determination of the growth direction of folds are applied in this study.
On an exemplarily examined idealized whaleback fold with an elliptical base it can bee figured out that the streams curve to maintain flow perpendicular to each contour line (Fig. 4a). The curvature of the stream depends on the elliptisity of the fold; the more circular the base the straighter the streams. Changes in the amplitude of the fold have no influence on the curvature of the rivers courses.
If the fold propagates laterally, an asymmetric forked drainage network starts to form. These drainage patterns develop by the inheritance of older tributary patterns in areas with less curvature around the top of folds and therefore may contain information about earlier stages of folding. This first generation of tributaries, more or less parallel to the fold axis, links with a second generation tributary pattern perpendicular to the fold flanks, always using the steepest available slope. These distinctive asymmetric tributaries can show lateral propagation directions as the flow direction of the older part of the linked tributaries show the growth direction.

With growing distance to the center of the fold the asymmetry of the tributary increases, finally resulting in curved tributaries at the nose of the fold, which only preserve the latest stages of the folding [Ramsey et al, 2008] (Fig. 4b).

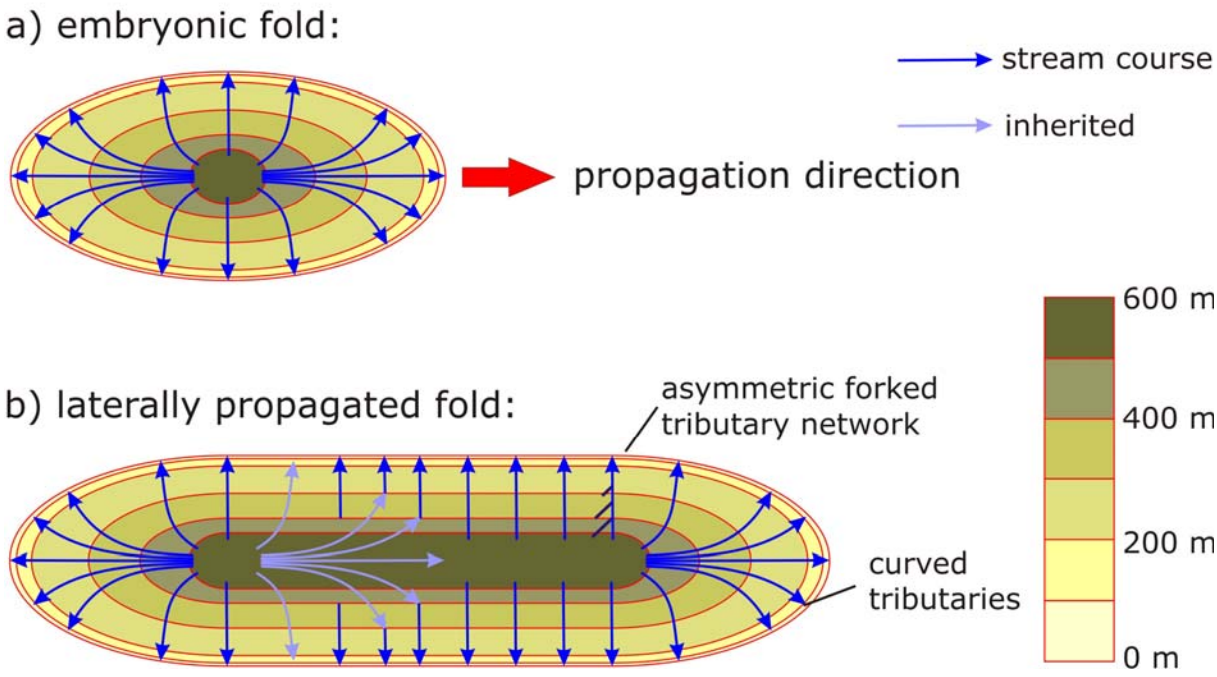

Figure 4: a) Map view with contour lines of an idealised embryonic cylindrical fold with its theoretical tributary pattern for an idealized fold with elliptical base and convex-up flanks. b) Tributary pattern for the same fold as above that has grown in length. First generation of tributaries, more or less parallel to the fold axis, links with the second generation tributary pattern perpendicular to the fold flanks, resulting in the development of asymmetric forked tributary networks. The nose of the fold shows curved tributaries.

Series of wind gaps formed by the same stream are an even stronger and easier visible feature to recognize lateral fold growth.

The development of wind gaps depends on the propagation and tectonic uplift rates of growing folds as well as on the incision rate of the river. If a fold starts to propagate laterally and the incision rate of the river is higher than the uplift rate of the fold a gorge, called water gap, establishes. If the incision rate of the river becomes lower than the uplift rate of the folds during further growth of the anticline, the river gets defeated and diverted leaving behind a dry valley called wind gap [Burbank et al., 1999; Burbank & Pinter, 1999]. Wind gaps show a distinctive convex-up long profile.

If two emerging folds join together it is possible that a river got pinched between the fold noses and forms a gorge in between. Because of the limited discharge through the narrow

outlet ponding of sediments behind the anticlines can form characteristic sediment depositions. (Fig. 5)

Figure 5 shows this evolution in a setting of two emerging anticlines combined with the processes discussed before and shown in Figure 4.

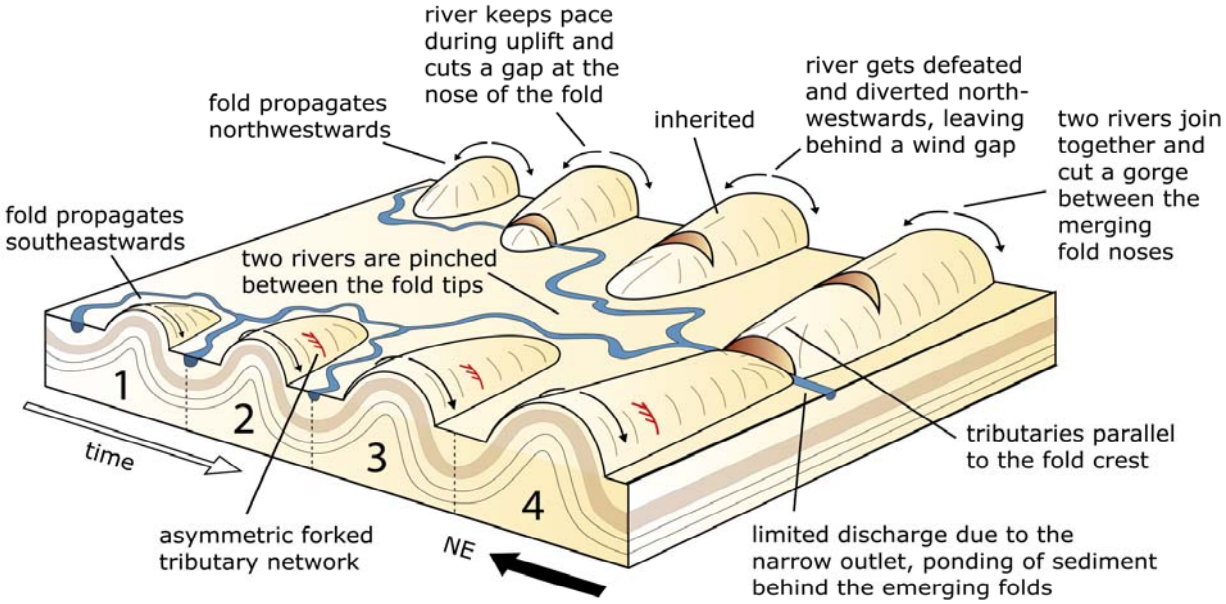

Figure 5: Schematic development of asymmetric forked tributary networks and wind gaps shows the development of a wind gap, the deflection and the pinching of a river between two propagating anticlines as a result of two emerging anticlines. First generation of tributaries links with the second generation tributary pattern perpendicular to the fold flanks. (strongly modified after L. A. Ramsey et al. (2008)).

3.3. New process: Curved wind gaps (Bretis)

During investigation a different form of wind gaps caught our attention. This kind of wind gaps, which have not been described in recent literature until present day, occur if uplift and lateral propagation rates of the growing fold exceed the incision rate of the river by far. Therefore large parts of the river course around the growing anticline are uplifted and now form a wind gap. In this study the new model of curved wind gaps is introduced (Fig. 6). These curved wind gaps are then often inherited by the new rising drainage system and therefore strongly influence it. In this case attention has to be paid using the asymmetric

forked tributaries to determine fold propagation directions because these curved wind gaps often change the appearance of the tributary patterns and so possibly lead to wrong results. Because of the appearance of curved wind gaps it is likely that river terraces occur in these dry river gorges. This leads to the assumption of the presence of material suitable for OSL (optically stimulated luminescence)-dating methods.

An additional step of investigation would be the gathering of samples in these curved wind gaps, to apply OSL-dating methods and to use the results of these data to quantify the propagation velocity especially of Bana Bawi anticline. Furthermore there may be possibilities to draw conclusions about propagation velocities of other growing anticlines in various areas.

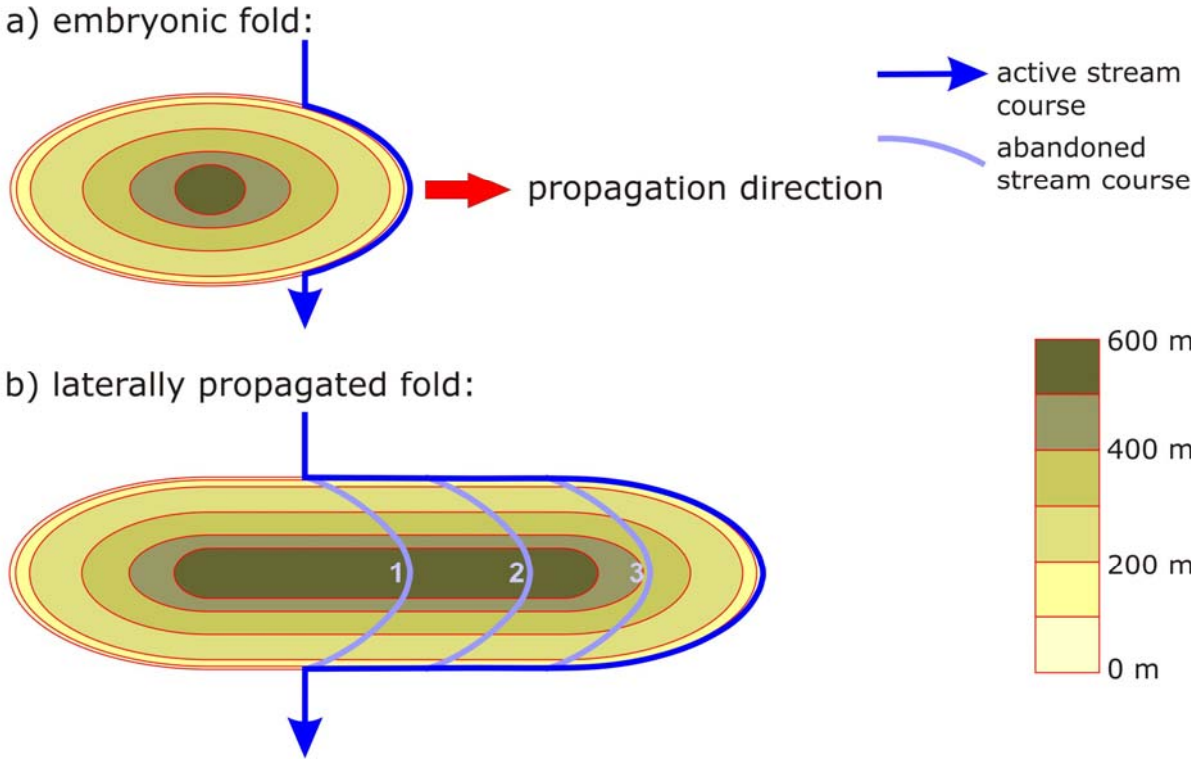

Figure 6: a) Map view with contour lines of an idealised embryonic cylindrical fold with elliptical base and convex-up flanks that deflects a river around the fold nose. b) Series of curved wind gaps due to very fast propagation and high tectonic uplift ratios of a fold growing in length

3.4. Development of hogbacks drawn on the example of Bana Bawi Anticline (Bretis)

The great differences in the strata cause the development of hogbacks and so have strong influence on the recent appearance of the investigation area. Hogbacks can be described as homoclinal ridges that form due to lithological contrasts and different weathering rates.
In the following sections the development of hogbacks will shortly be described drawn on the example of Bana Bawi Anticline:

The development of hogbacks can be described as continuous process which starts in an early stage of fold growth. In particular the process starts at ongoing shortening and uplift with simultaneous erosion of the overlying sediments. In case of Bana Bawi Anticline the overlying Bakhtiari sediments, containing conglomerate, sandstone and claystone started to get eroded. Due to the whaleback-like form of Bana Bawi Anticline it came to a rapid exposure of large areas of the flat crest which caused strong erosion on top of the Anticline. On the flat crest the erosion progressed rapidly due to the reason that shallow dipping layers experience stronger erosion than steep layers. Furthermore in areas with high curvature the appearance of higher fracture densities causes stronger erosion than in areas with lower curvatures and fracture densities. Consequently an embryonic basin started to form in the centre of Bana Bawi Anticline.
At todays erosion level competent layers form steep cliffs at the margin of the Bana Bawi anticline. These cliffs are built up by Pilaspi Formation which mainly consists of well bedded limestone with low fracture densities.
The underlying Kolosh, Tanjero and Shiranish Formations consist of sandstones, siltstones, claystone, marls as well as limestone with high fracture densities.
Therefore these formations are eroded much faster, which causes the exposure of the underlying massive Aqra-Bekhme limestone and dolomites that form the topographic culmination in the centre of the anticline (Fig. 7).

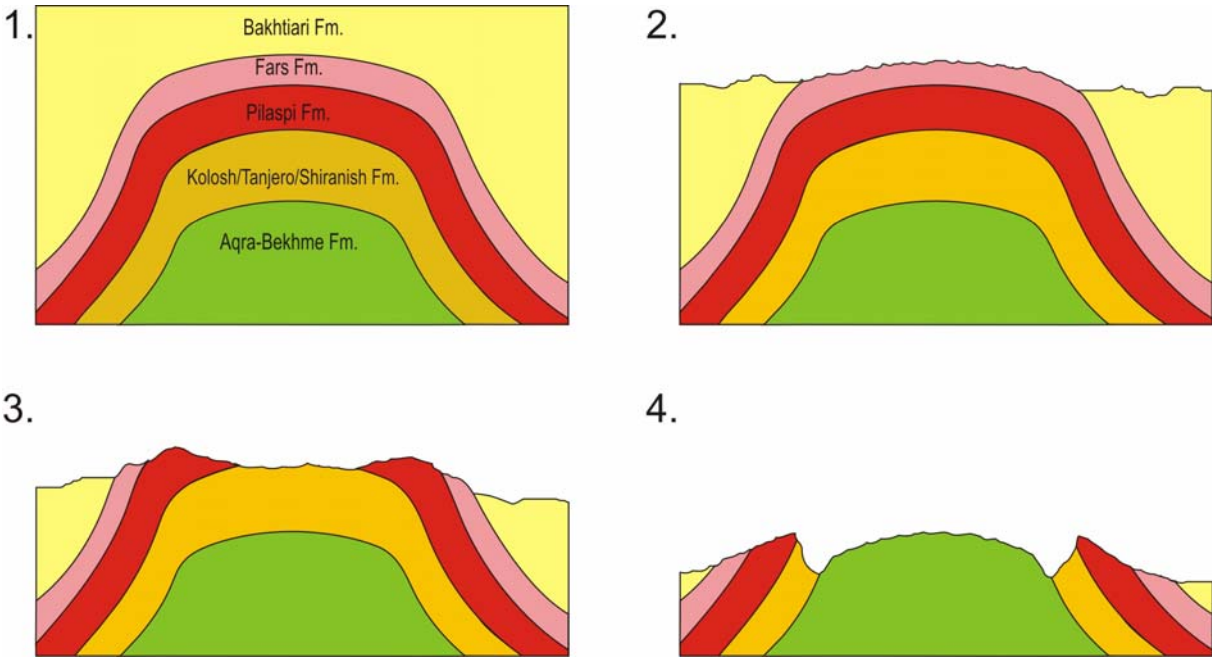

Figure 7: 1. Cross section normal to the fold axis of Bana Bawi-Anticline buried by Bakhtiari sediments; 2. Bakhtiari sediments are eroded; rapid exposure of large areas of the flat crest of Bana Bawi Anticline; strong erosion on top of the Anticline; 3. Rapid erosion of the flat crest; an embryonic basin starts to be formed in the centre of Bana Bawi Anticline; 4. Competent layers form steep cliffs at the margin and the topographic culmination in the centre of the anticline of Bana Bawi anticline

3.5. Quantification of geomorphologic parameters (Bartl/Bretis)

Selected geomorphologic parameters, such as the spacing ratio, R, the basin elongation ratio, B_s, the circularity index, C and the basin shape, R_f, can be used to characterize the tectonic activity and basin maturity of certain regions.

Observations of topographic maps indicate that the spacing of drainage basin outlets often shows very constant values along mountain fronts [Mayer, 1986; Talling et al, 1993; 1997]. High spacing ratios indicate high rates of tectonic activity, while lower spacing ratios indicate lower rates of active tectonics. It is expressed as:

$$R = W / S,$$

where W is the half-width, measured from the mouth of the basin to the main drainage divide perpendicular to the mountain front and S is the spacing between two mouths (Fig. 8a). For this study only drainage networks which extend over 80% of the distance between mountain front and main drainage divide where chosen. Similar studies, such as Hovius (1996) and

Talling (1997), use distances of 70% (Talling) and 90% (Hovius). Furthermore areas influenced by wind gaps or other structures (i.e. roads that influenced the morphology of channels extracted in Rivertools 3.0) were excluded. Drainage basins with confluences less than 2% of the way from the mountain front to the main drainage divide were treated separately. Additionally, due to limited resolution of the DEM, only basins whose straight distance from the mountain front to the main drainage divide exceeds 1000 m were included in statistics.

The elongation ratio of the drainage basins is another useful indicator to characterize the tectonic activity of a mountain range area. Elongated basins occur in active areas while more circular basins form after cessation of mountain uplift [Bull and McFadden, 1977]. It is expressed as:

$B_s = B_l / B_w$,

where B_l is the length of the basin from its mouth to the most distal point and B_w is the width of the basin. Recent literature [i.e. Bull and Mc Fadden, 1977; Hovius,1996; Talling et al, 1997; Ramirez-Herrera, 1998; Burbank & Anderson, 2001; Tsodoulos et al, 2008] does not explicitly describe how to measure these distances. This fact causes problems mainly at measuring curved basins. Therefore a specially adapted method is used for this study. B_l is measured from the mouth of the basin to the most distal point in the drainage divide. As long as a straight line between these two points does not cross the drainage divide the distance is measured as a straight line (Fig. 8b). If the straight line between these two points crosses the drainage divide, the distance is measured as a curved line which runs along the centre of the basin to the most distal point of the main drainage divide (Fig. 8c). In both cases B_w is measured perpendicular to B_l through its midpoint (Fig. 8b and 8c).

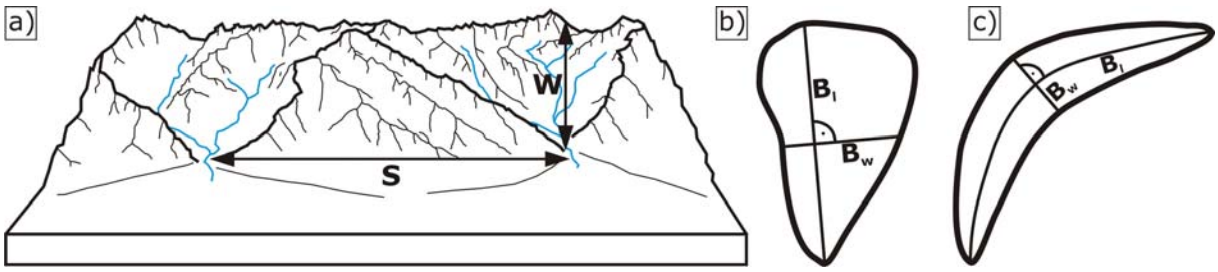

Figure 8: a) Two mountainous catchments. W is the half width a drainage basin, defined as the distance from the mountain front to the main drainage divide and S is the distance between the outlets of two catchments (modified after Hovius (1996)). b) Drainage basin where B_l is a straight line between the mouth of the basin and the most distal point on the drainage divide and B_w is a straight line perpendicular

through the midpoint of B_l. c) Curved drainage basin where B_l is a curved line between the mouth of the basin and the most distant point on the drainage divide and B_w is a straight line perpendicular through the midpoint of B_l.

The circularity index expresses the area of a circle to the area of the basin using the same perimeter length [Bell, 2004].
Dendritic basins need more time to develop and represent more mature areas. The circularity index of such basins is higher than of more elongated basins. It is defined as:

$$C = A_b / A_c,$$

where A_b is the area of the basin and A_c is the area of a circle with the same length of perimeter (P) as the basin.
An additional index, which correlates with the elongation ratio and the circularity index, is the basin shape. It describes how squarish the shape of a basin is. Hence:

$$R_f = A_b / B_l^2,$$

where A_b is the area of the basin and B_l is the length of the basin as mentioned previously.
These parameters were calculated for every individual basin. For each investigated segment the mean values (R', B_s', C', R_f') were calculated. Furthermore R'', B_s'', C'' and R_f'' were calculated out of the means of the measurements. The values of R' and B_s' are generally greater than the values of R'' and B_s''. This discrepancy is due to the mean value of 1/S being greater 1/S' and $1/B_w$ being greater than $1/B_w$', where S' is the mean value of S and B_w' is the mean value of B_w. The mean value of W/S is therefore greater than the ratio of the mean values of W'/S' and the mean value of B_l/B_w is greater than the ratio of the mean values of B_l'/B_w' [Talling, 1997].
Additional parameters extracted for each basin are the longest channels length (km), its vertical drop (m), its slope (m/m) and its sinuosity (m/m).
For all the mentioned parameters and ratios also the median and standard deviation (in %) where calculated.

4. Results

4.1. Geomorphologic criteria and Growth quantification (Bartl/Bretis)

The investigation area, consisting of Bana Bawi, Permam and Safeen Anticlines, is situated in Kurdistan region of northeastern Iraq, approximately 25 km northeast of the city of Erbil. It covers about 1000 km² in the Zagros simply folded belt (Fig. 9).

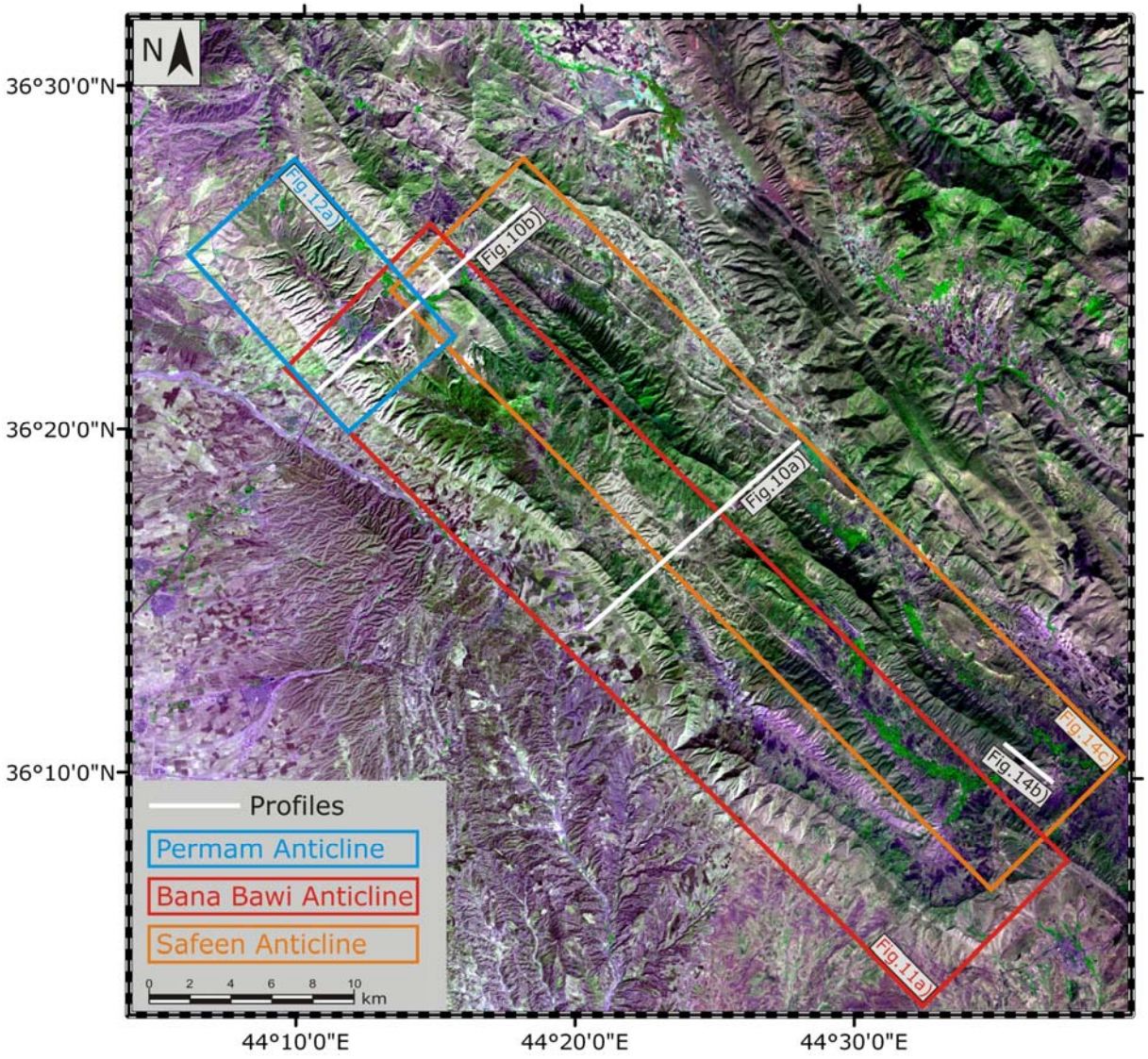

Figure 9: False colour composite satellite image of the investigation area northeast of the city of Erbil; blue: Permam Anticline; red: Bana Bawi Anticline; orange: Safeen Anticline; white: profiles

Hydrologically, there are few rivers with perennial flow conditions and therefore the dominant fluviatile erosion mainly takes place in the months with periodical precipitation, which varies between 700 and 3,000 mm/yr (i.e. during the winter months).
The Bana Bawi, Permam and Safeen Anticlines form NW-SE striking fold chains over an exposed distance of more than 70 km. The dominant wavelength of the fold chains is between 6 km (Safeen Anticline) and 8 km (Bana Bawi Anticline).
Along the limbs of these Anticlines, Cretaceous to Tertiary sediments are exposed consisting of competent lithologies such as well bedded to massive limestone, dolomites and sandstones, intercalated with incompetent lithologies such as marls and claystone (Fig. 2).
These differences in strata strongly influence the recent appearance of the three anticlines. More competent layers (e.g. Pila Spi and Bekhme Formation) show stronger resistivity to erosion and hence form the hogbacks as well as the topographic culminations in the center of the anticlines.
Less competent layers (e.g. Shiranish and Kolosh Formation) are strongly eroded and can partly be found in the depressions of the inner part of the anticlines.
The forelimb of the Bana Bawi – Permam fold train has a mean dip of approximately 45° towards SW.
The backlimb dips about 35° to the NE, but due to erosion and accessibility reliable measurements were only possible at Permam Anticline.
The limbs of the Safeen anticline dip by approximately 55° towards NE (backlimb) and 60° towards SE (forelimb).
Based on the field measurements two line-length and area balanced cross sections (Fig. 10) were drawn perpendicular to the fold axis using the constant dip method [Faill, 1969, 1973; Laubscher, 1977; Suppe, 1983; Suppe & Chang, 1983]. These profiles are the basis for the approximate calculation of the detachment depth in the investigation area. Therefore we used the equal area equation $D_c=A_f / (L_f-L_1)$ [Ramsay & Huber, 1983; Homza et al, 1995] to calculate the constant detachment depth, D_c assuming an ideal detachment fold. A_f is the uplifted area; L_f the arc length of reference and L_1 the length of the bed after folding. Using this method a likely detachment horizon for Bana Bawi, Permam and Safeen Anticlines was calculated in a depth between 4.6 and 5.3 km.

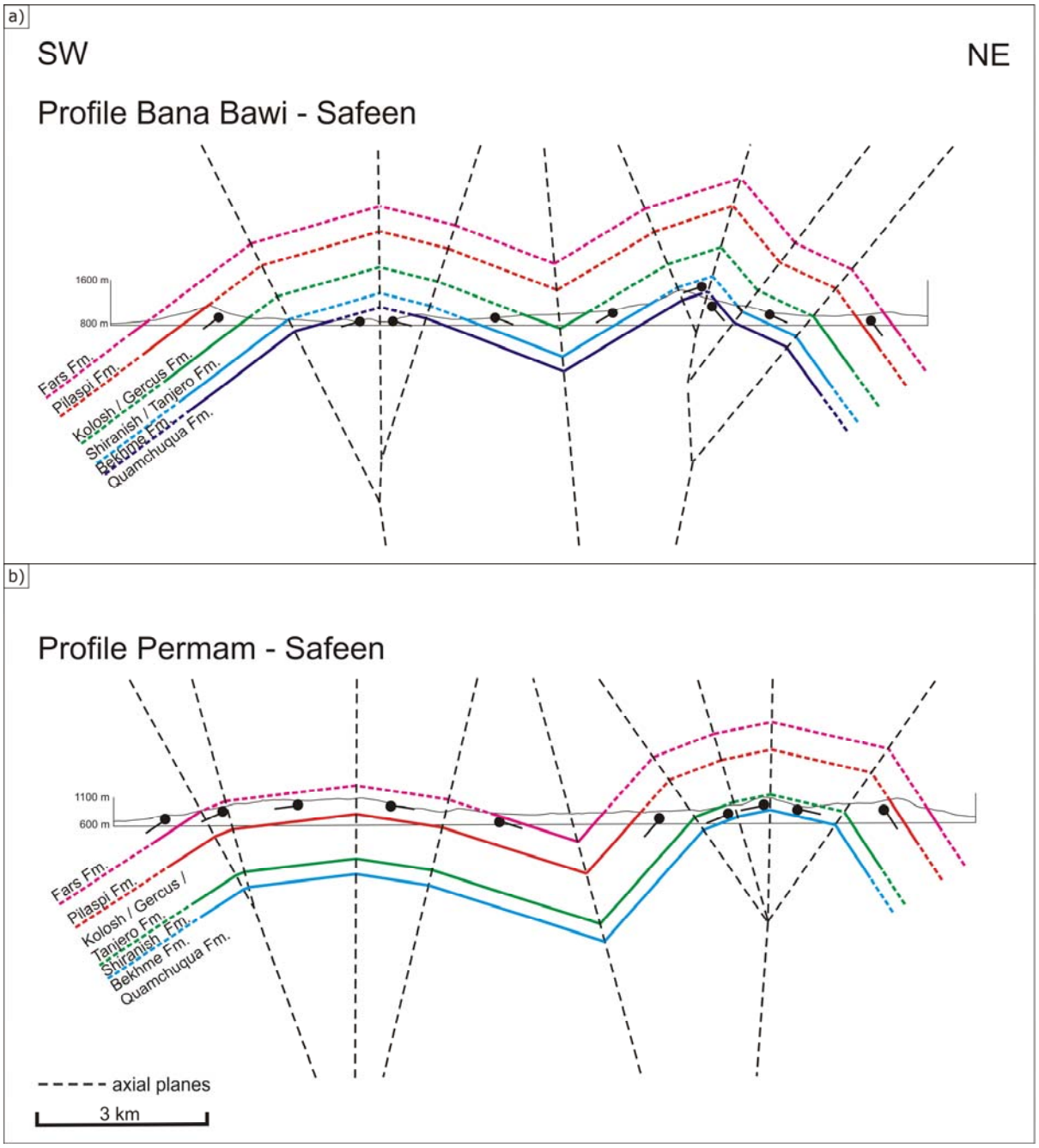

Figure 10: a) Line-length and area balanced profile perpendicular to the fold axis of Bana Bawi and Safeen Anticlines; b) Line-length and area balanced profile perpendicular to the fold axis of Permam and Safeen Anticlines (positions shown in Fig. 9)

4.1.1. Bana Bawi and Permam Anticlines (Bretis)

At first glance the Permam-Bana Bawi fold train seems to be a single contiguous fold, whose appearance is related to lithological differences. However, tectono-geomorphological investigations show that it consists of several segments that initially started to amplify as individual structures and joined during lateral propagation.
Indicators therefore are the presence of wind gaps, the pattern of deflected rivers and fanned drainage patterns, which, in the cylindrical parts of the fold are strongly overprinted by transverse rivers perpendicular to the fold axis.
Bana Bawi Anticline (location see Fig. 9) shows a lot of excellent examples to quantify its lateral propagation (Fig. 11). Its shape is dominated by the southwestern hogback and the topographic culmination in the core of the anticline. Following the course of the hogback shows that it forms an edge around Bana Bawi - as well as Safeen Anticline.
The course of the hogback rim and the very narrow space between Safeen- and Bana Bawi Anticline indicate that these anticlines show a complex higher order fold interference pattern.
Permam Anticline is a part of the rim around the anticlines but does not form a hogback. It seems to be younger and thus shorter exposed to erosion, which can be detected due to its nearly flawless whaleback form.

4.1.1.1. Bana Bawi Anticline

Due to strong erosion most of the drainage patterns of the hogback itself cannot be used to determine the fold propagation directions. Only in the northwestern most part, where the erosion of the fold crest is less progressed, statements regarding the evolution can be made (Fig. 11c). In this area the drainage system of the forelimb is characterized by fanned tributaries which, from a central point, clearly suggest a growth direction towards the northwest. Towards the center the pattern straightens and then turns around when the growth direction of the fold segment changes towards southeast.
A topographic profile (Fig. 11b) along the fold crest in the southeastern part of the anticline shows a decrease in relief from the center towards northwest and southeast. Furthermore it shows the decrease in the topographic height of the wind gaps, the younger they are.
The area around the northwestern part of the profile is characterized by three rivers which can be used to determine the growth history within in it (Fig. 11d). Rivers A and B are deflected

towards southeast while river C is deflected towards northwest before they cross the fold. River A forms a water gap and river C is pinched in between the two joining fold segments. In the southeastern part of the anticline two generations of wind gaps can be distinguished. The older generation was formed by rivers that drained towards the southwest in an earlier stage of fold growth. The center of the fold segment, from where propagation started is suggested to be in between the curved wind gap in the northwest and the two wind gaps southeast of it (Fig. 11a). This old wind gaps (especially the curved wind gap) had strong influence on the development of the new rising drainage pattern and its occurrence. Therefore care has to be taken by using the fanned drainage network to quantify the fold growth directions.

Continuous uplift, propagation and erosion of the fold segment had strong influence on geomorphology and topology of the area. For that reason changes in the main drainage system took place. A new river started to drain towards the southeast which led to the formation of a series of younger wind gaps in the area around the southeastern fold nose. Due to fast fold propagation and high uplift rates, this younger generation occurs as curved wind gaps. Therefore large parts of the river course along the forelimb of the core of Bana Bawi Anticline have been uplifted.

This series of curved wind gaps with decreasing topographic height towards southeast is a strong indicator for a fold growth in southeastern direction (Fig. 11e + 11f).

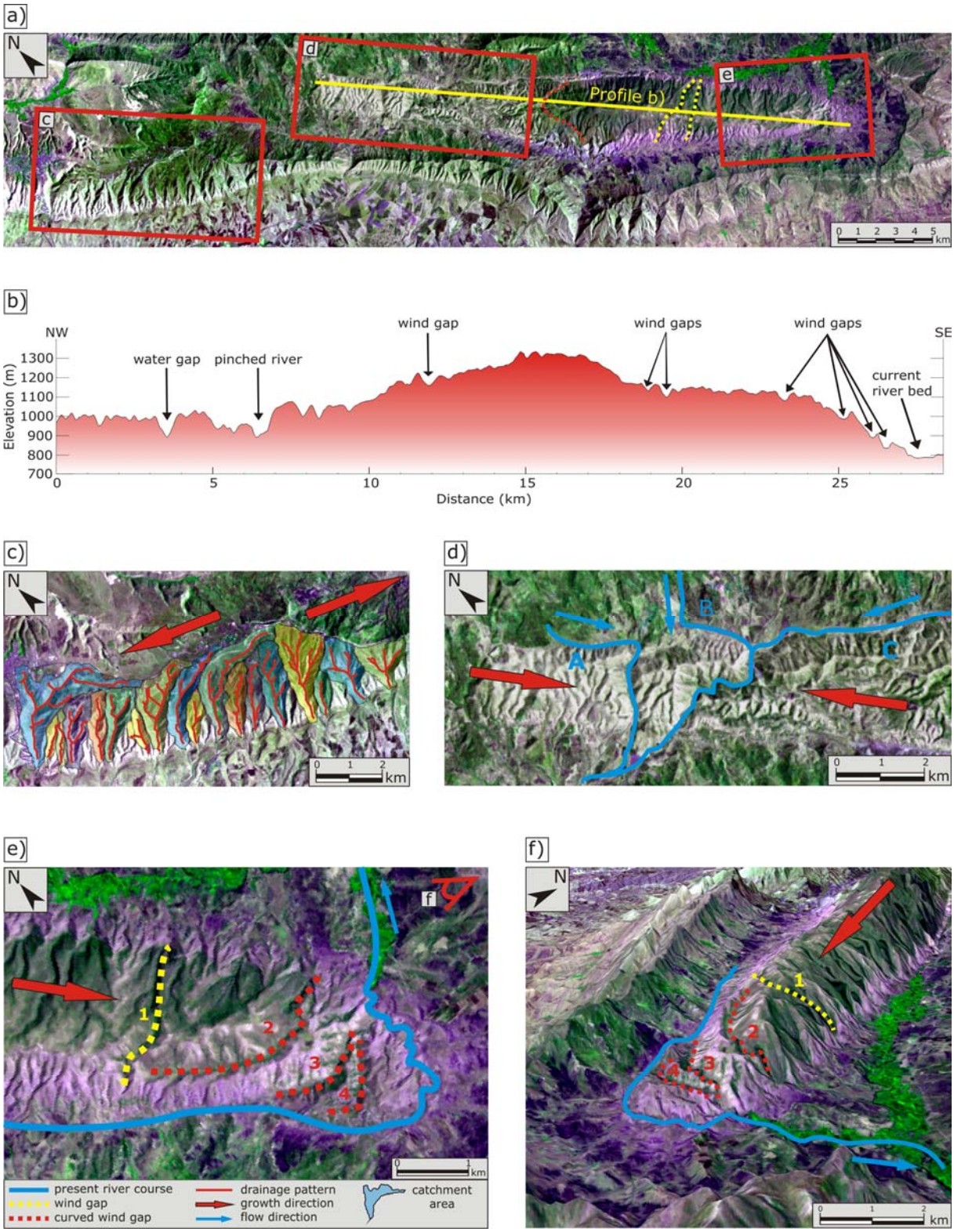

Figure 11: location shown in Figure 9; a) 30m ASTER false colour overview of Bana Bawi Anticline; the yellow line shows the position of Profile b); the red rectangles show the positions of c), d) and e); the red (curved) and yellow dotted lines are showing wind gaps that are not shown in the figures below; b) Topographic profile for the 30m ASTER DEM along the fold crest of Bana Bawi Anticline showing a decrease in relief towards the noses of the fold segment, the current rivers crossing the anticline as well as a number of wind gaps with decreasing height at decreasing age; c) asymmetric forked drainage patterns and their catchment areas as indicators for growth directions on the NW part of the forelimb of Bana Bawi Anticline; d) pinched and deflected rivers in the centre of Bana Bawi Anticline as indicator for growth directions; e) curved wind gaps on the SE fold nose of the core of Bana Bawi Anticline that show

the direction of propagation; f) 3D view of the core of Bana Bawi Anticline and its curved wind gaps (location shown in e));

4.1.1.2. Permam Anticline

Permam Anticline (location see Fig. 9) forms an almost perfect example of a whaleback fold segment whose growth can be determined by an asymmetric forked tributary pattern. Due to the reason that only limestone of the Pilaspi Formation crops out on the entire fold segment, lithological differences as factors influencing the appearance of the tributary patterns can be excluded. The tributaries on the northwestern part of the anticline curve towards the southeast, whereas the tributaries on the southeastern part show asymmetries towards the northwest. In the centre the river courses are straight down slope perpendicular to the fold axis (Fig 12a). Another indicator for Permam being an individual fold segment is the decrease in relief from the centre of the fold towards northwest and southeast where it links with one of the Bana Bawi fold segments. This linkage becomes evident regarding the lower slope towards Bana Bawi (Fig. 12b).

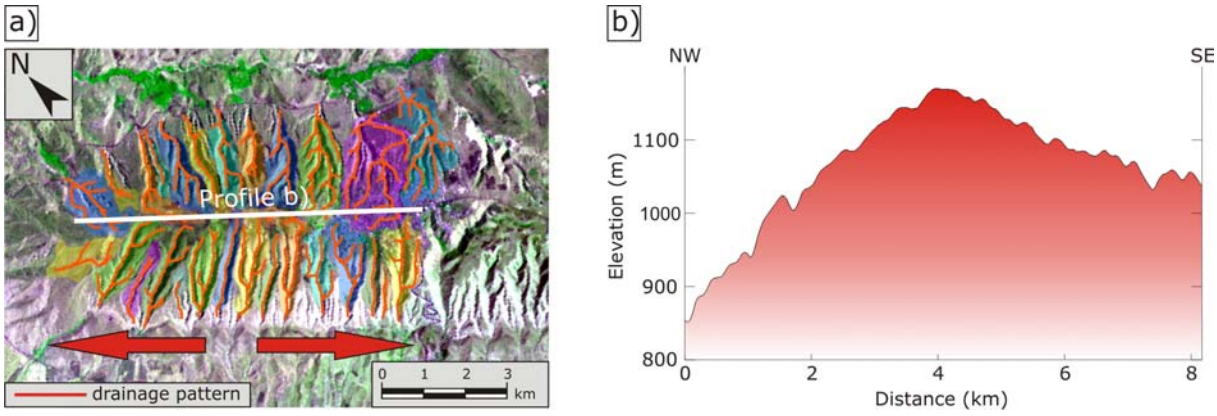

Figure 12: location shown in Figure 9; a) forked tributary patterns of Permam Anticline and its catchment areas; the asymmetry decreases towards the centre of the fold and shows the growth directions towards the NW and SE; b) Topographic profile along the fold crest with decreasing height by increasing distance to the centre (position see Figure a))

All these geomorphic criteria suggest that the Bana Bawi – Permam fold train is compound by three individual fold segments that joined during lateral propagation (Fig. 13). Due to the status of erosion it can be estimated that Permam Anticline is the youngest of these three segments. The deflection of the river and the presence of a series of wind gaps in the

southeastern part of the core of Bana Bawi Anticline lead to the assumption that the fold growth is still continuing at high rates of lateral propagation.

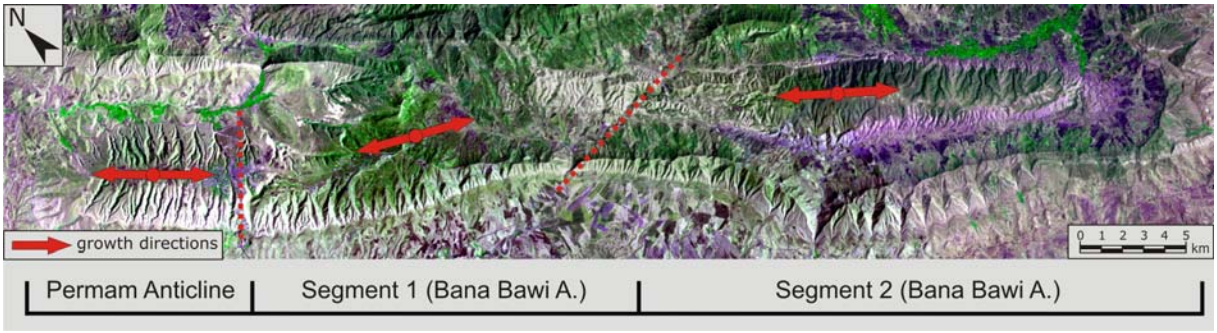

Figure 13: Bana Bawi – Permam fold chain with its three individual segments that joined together during lateral propagation.

4.1.2. Safeen Anticline (Bartl)

The earlier mentioned hogback, which rims Bana Bawi- and Safeen Anticline, is eroded down to a ridge of about 100m height in this area and thus can not be used to determine and quantify lateral fold propagation. Therefore this study concentrates on the core of Safeen Anticline, which shows us many different examples to investigate the behavior of lateral fold propagation (Fig. 14a).

The kinks of Safeen Anticline (Fig. 9) indicate that the fold comprises more than only one segment.

Interestingly the erosional signatures differ significantly along the backlimb as well as along the forelimb. Both limbs are dominated by transverse river segments and partially record straight almost perpendicular to the fold axis with a spacing of the basins between about 200 and 600 m.

Asymmetric forked tributary networks can be found all over the anticline, providing excellent indicators for lateral growth directions.

A water gap in the southeast of the fold indicates a growth in southeastern direction. If the fold growth is going to exceed the incision rate in the future this water gap would represent a possible wind gap.

A wind gap, located in the midsection of the fold, shows a possible linkage of two segments, which caused the pinching of a river in this area (Fig. 14a and 14b).

Some patterns are straightened and contain almost parallel tributaries, which can be interpreted as inflexion points of the growth directions (Fig. 14a).
All these observations can be conducted to the assumption, that Safeen Anticline comprises four individual fold segments which joined together during lateral propagation (Fig. 14c).
A relative age sequence of the four segments building Safeen Anticline was done interpreting higher order folds in the hinge area of the fold as well as the appearance of the tributaries. Figures 14d and 14e show 11 profiles perpendicular to the fold axis. The northwestern part of the hinge is dominated by a higher order M-fold as well as curved channels and high incision rates. In contrast the southeastern part of the fold is dominated by straighter channels and lower incision rates. These observations lead to the assumption of an increasing age in northwestern direction.

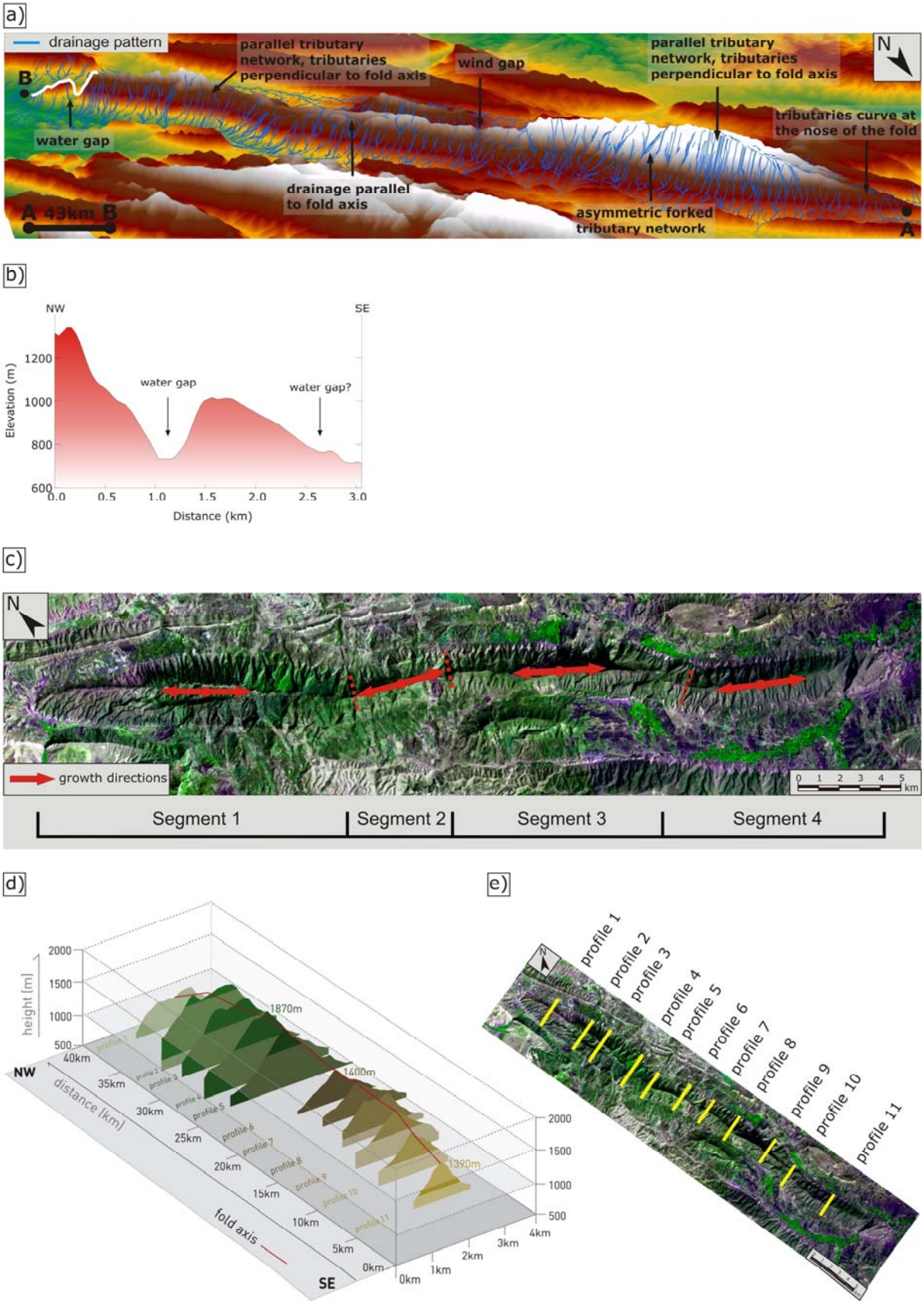

Figure 14: location shown in Figure 9; a) Safeen Anticline overlaid by a digital river network (generated using a 30m ASTER DEM); the white line is the profile line of Profile b); b) Topographic profile for the 30m ASTER DEM along the SE part of the fold crest of Safeen Anticline showing a decrease in relief towards the nose of the fold as well as a recent water gap; c) Safeen anticline with its four individual segments that joined together during lateral propagation; d) 3D arrangement of 11 profiles located as

shown in Figure e) perpendicular to the fold axis along Safeen Anticline; e) position of the 11 profiles along Safeen Anticline used in Figure d);

4.2. Quantification of geomorphologic parameters (Bartl/Bretis)

The quantification of geomorphologic parameters is a powerful method to characterize differences in tectonic activity and basin maturity in various areas. In this study the spacing ratio (R), the elongation ratio (B_s), the circularity index (C) and the basin shape (R_f) were calculated for 250 drainage basins in the investigation area (Fig. 15) to figure out differences in the rates of the tectonic activity between the different fold segments. Additionally differences in the morphology of fore- and backlimbs were analyzed. The values for the ratios and parameters discussed in the following can be found in Table 1 in the appendix.

Permam Anticline forms a whaleback with a forelimb dipping around 45° towards SW and a backlimb dipping around 35° towards NE. Differences in the shape of the drainage network (Fig. 15b) occur with higher sinuosities and wider channel spacing along the backlimb in contrast to the forelimb.
In the NW part of Bana Bawi Anticline (Fig. 15c) convenient values could only be extracted from the forelimb because the appearance of the backlimb is strongly influenced by the neighboring Safeen Anticline. The results of the forelimb are very similar to those extracted on the forelimb of Permam Anticline which indicates a similar tectonic activity in this part of the investigation area.
Due to the different erosion level the values reached from the hogback (Fig. 15d-f) have to be treated separately and cannot be compared with Permam Anticline and the northwestern part of Bana Bawi Anticline. Nevertheless R and B_s show an increasing trend towards the SE whereas the values for C and R_f drop in this direction. These results indicate an increasing tectonic activity and consequential lower basin maturity in southeastern direction. This statement is supported by the appearance of curved wind gaps in the southeastern most part of Bana Bawi Anticline.
The forelimb of the core of Bana Bawi Anticline shows a narrower spacing and lower sinuosities in contrast to the backlimb, whereas the slope of the channels on both limbs is very similar. R and B_s are higher on the forelimbs while consequently C and R_f are higher on the

backlimbs. The high elongation and spacing ratios on the core of Bana Bawi Anticline substantiate the statement of increasing tectonic activity towards SE.

The first segment of Safeen Anticline (Fig. 15h) is characterized by lithological differences. In the northwestern part of this segment the outcropping of Bekhme formation leads to a drainage pattern with narrower spacing and consequently more elongated basins. This behavior could only be analyzed on the backlimb, because due to the high order fold on the forelimb the drainage basins are distorted and moreover they are too short to extract useful values for quantification.
Due to the narrow spacing certain basins on the backlimb show an extreme elongation which causes the high values of R and B_s in this area. In the southeastern part of this segment, where Qamchuqa Formation is outcropping, the values drop significantly. Consequently the values of C and R_f show an opposing trend.
Similarly to Bana Bawi Anticline, R and B_s show an increasing trend towards the SE whereas the values for C and R_f drop in this direction, with the exception of the slightly opposing trend between the segments in j and k (Fig15j-k).
These results indicate an increasing tectonic activity and a lower basin maturity in southeastern direction.

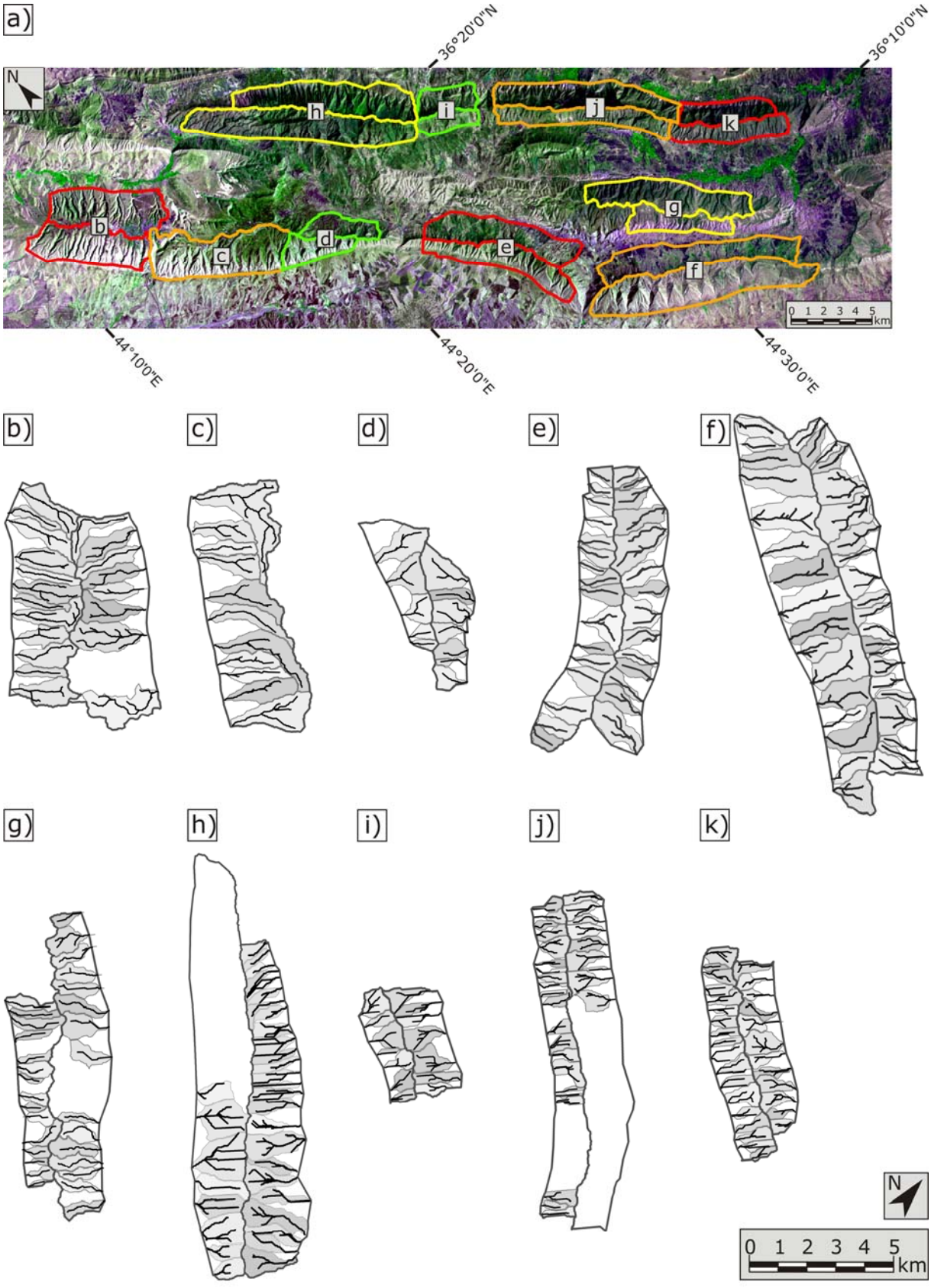

Figure 15: Location of the different fold segments (a) used for quantification and their individual basins as well as the courses of the main streams (b-k)

5. Conclusion (Bartl/Bretis)

The use of geomorphologic criteria leads to the result that the structure of the investigated folds follows a complex pattern.

This study demonstrates that the anticlines have developed from several embryonic folds, which have merged during lateral propagation and form extended fold trains.

The merging points of the individual fold segments have major effects on the pattern of the regional drainage system. All along the investigated anticlines, direct evidence for lateral propagation in form of distinctive drainage patterns and wind gaps can be found.

As a special form of wind gaps, the new model of “curved wind gaps” was determined. This form of wind gaps develops in areas with high tectonic uplift and propagation rates with simultaneous low incision rates.

In detail the Permam-Bana Bawi fold train comprises three different fold segments that joined during lateral propagation, whereas Safeen Anticline is built up by four different fold segments.

As a further step of investigation various geomorphologic parameters, describing tectonic activity and basin maturity, where analyzed.

The shape of the drainage basins is strongly influenced by lithological contrasts, whereas the orientation of bedding and jointing has no significant influence on their appearance.

The spacing of the drainage basins is very constant over different areas.

The interpretation of the calculated geomorphologic ratios indicates a high tectonic activity of the region and a low maturity of the drainage basins, with a slightly opposing trend towards the Northwest, which is also highlighted by the occurrence of curved wind gaps in the south-eastern part of the investigated area.

6. References

ALLEN, M.B., JONES, S., ISMAIL-ZADEH, A., SIMMONS, M. & ANDERSON, L. (2002) Onset of Subduction as the Cause of Rapid Pliocene-Quaternary Subsidence in the South Caspian Basin. *Geology*, **30,** 775-778.

BELL, F.G. (2004) *Engineering Geology and Construction*. Spon Press, New York.

BERBERIAN, M. (1995) Master Blind Thrust Faults Hidden under the Zagros Folds: Active Basement Tectonics and Surface Morphotectonics. *Tectonophysics*, **241,** 193-224.

BULL, W.B. & MCFADDEN, L.D. (1977) Tectonic Geomorphology North and South of the Garlock Fault, California. In: *Proceedings of Eighth Annual Geomorphology Symposium, Geomorphology in Arid Regions* (Ed. by D. O. Doehring), 115–138. State University of New York, Binghamton.

BURBANK, D.W., MCLEAN, J.K., BULLEN, M., Y., A.K. & MILLER, M.M. (1999) Partitioning of Intermontane Basins by Thrust-Related Folding , Tien Shan, Kyrgyzstan. *Basin Research*, **11,** 75-92.

BURBANK, D.W. & PINTER, N. (1999) Landscape Evolution: The Interactions of Tectonics and Surface Processes. *Basin Research*, **11,** 1-6.

BURBANK, D.W. & ANDERSON, R.S. (2001) *Tectonic Geomorphology*. Blackwell Science Malden, MA, USA.

BURBERRY, C.M., COSGROVE, J.W. & LIU, J.G. (2008) Spatial Arrangement of Fold Types in the Zagros Simply Folded Belt, Iran, Indicated by Landform Morphology and Drainage Pattern Characteristics. *Journal of Maps***,** 417-430.

COOPER, M. (2007) Structural Style and Hydrocarbon Prospectivity in Fold and Thrust Belts: A Global Review. In: *Deformation of the Continental Crust: The Legacy of Mike*

Coward (Ed. by A. C. Ries, R. W. H. Butler & R. H. Graham), 447-472. The Geological Society of London, Special Publication, London.

DAVIS, A.M., LIU, J.G. & BROWN, M.A.N. (2003) Drainage Development Related to Blind Thrust Evolution Along the Flaming Mountain, Turpan Basin, Xinjiang, Nw China. *Geoscience and Remote Sensing Symposium*, **5,** 3326-3328.

DAVIS, K., BURBANK, D.W., FISHER, D., WALLACE, S. & NOBES, D. (2005) Thrust-Fault Growth and Segment Linkage in the Active Ostler Fault Zone, New Zealand. *Journal of Structural Geology*, **27,** 1528–1546.

DELCAILLAU, B. (2001) Geomorphic Response to Growing Fault-Related Folds: Example from the Foothills of Central Taiwan. *Geodinamica Acta*, **14,** 265–287.

DELCAILLAU, B., CAROZZA, J.M. & LAVILLE, E. (2006) Recent Fold Growth and Drainage Development: The Janauri and Chandigarh Anticlines in the Siwalik Foothills, Northwest India. *Geomorphology*, **76,** 241-256.

DERCOURT, J., ZONENSHAIN, L.P., RICOU, L.-E., KAZMIN, V.G., LE PICHON, X., KNIPPER, A.L., GRANDJACQUET, C., SBORTSHIKOV, I.M., GEYSSANT, J., LEPVRIER, C., PECHERSKY, D.H., BOULIN, J., SIBUET, J.-C., SAVOSTIN, L.A., SOROKHTIN, O., WESTPHAL, M., BAZHENOV, M.L., LAUER, J.P. & BIJU-DUVAL, B. (1986) Geological Evolution of the Tethys Belt from the Atlantic to the Pamirs since the Lias. *Tectonophysics*, **1-4,** 241-315.

DEWEY, J.F., PITMAN, W.C., RYAN, W.B.F. & BONNIN, J. (1973) Plate Tectonics and the Evolution of the Alpine System. *Geological Society of America Bulletin*, **84,** 3137-3180.

FAILL, R.T. (1969) Kink Band Structures in the Valley and Ridge Province, Central Pennsylvania. *Bulletin of the Geological Society of America*, **84,** 2539-2550.

FAILL, R.T. (1973) Kink-Band Folding, Valley and Ridge Province, Pennsylvania. *Bulletin of the Geological Society of America*, **84,** 1289-1314.

GARBRECHT, J. & MARTZ, L.W. (1997) The Assignment of Drainage Direction over Flat Surfaces in Raster Digital Elevation Models. *Journal of Hydrology*, **193,** 204-213.

HILLEY, G. & ARROWSMITH, J.R. (2008) Geomorphic Response to Uplift Along the Dragon's Back Pressure Ridge, Carrizo Plain, California. *Geology*, **36,** 367-370.

HOMKE, S., VERGÉS, J., GARCÉS, E., M. H. & KARPUZ, R. (2004) Magnetostratigraphy of Miocene Pliocene Zagros Foreland Deposits in the Front of the Push-E Kush Arc (Lurestan Province, Iran). *Earth and Planetary Science Letters*, **225,** 397-410.

HOMKE, S., VERGÉS, J., SERRA-KIEL, J., BERNAOLA, G., SHARP, I., GARCÉS, M., MONTERO-VERDÚ, I., KARPUZ, R. & GOODARZI, M.H. (2009) Late Cretaceous–Paleocene Formation of the Proto–Zagros Foreland Basin, Lurestan Province, Sw Iran. *Geological Society of America Bulletin*, **121,** 963-978.

HOMZA, T.X. & WALLACE, W.K. (1995) Geometric and Kinematic Models for Detachment Folds with Fixed and Variable Detachment Depths. *Journal of Structural Geology*, **17,** 475-488.

HOVIUS, N. (1996) Regular Spacing of Drainage Outlets from Linear Mountain Belts. *Basin Research*, **8,** 29-44.

JACKSON, J., NORRIS, R. & YOUNGSON, J. (1996) The Structural Evolution of Active Fault and Fold Systems in Central Otago, New Zealand: Evidence Revealed by Drainage Patterns. *Journal of Structural Geology*, **18,** 217-234.

JACKSON, J., VAN DISSEN, R. & BERRYMAN, K. (1998) Tilting of Active Folds and Faults in the Manawatu Region, New Zealand: Evidence from Surface Drainage Patterns, New Zealand. *Journal of Geology and Geophysics*, **41,** 377-385.

JASSIM, S.Z. & BUDAY, T. (2006) Units of the Unstable Shelf and the Zagros Suture. In: *Geology of Iraq* (Ed. by S. Z. Jassim & J. C. Goff), 71-83. Prague and Moravian Museum, **Brno**.

JASSIM, S.Z. & GOFF, J.C. (2006) Phanerozoic Development of the Northern Arabian Plate. In: *Geology of Iraq* (Ed. by S. Z. Jassim & J. C. Goff), 32-44. Prague and Moravian Museum, Brno.

KELLER, E.A., GURROLA, L. & TIERNEY, T.E. (1999) Geomorphic Criteria to Determine Direction of Lateral Propagation of Reverse Faulting and Folding. *Geology*, **27,** 515-518.

LAUBSCHER, D.H. (1977) Geomechanics Classification of Jointed Rock Masses—Mining Applications. *T. I. Min. Metall,* **A 86,** A1-A8.

MAYER, L. (1986) Tectonic Geomorphology of Escarpment and Mountain Fronts. In: *Active Tectonics* (Ed. by R. E. Wallace), 125-135. National Academy of Science, USA.

MCQUARRIE, N., STOCK, J.M., VERDEL, C. & WERNICKE, B.P. (2003) Cenozoic Evolution of Neotethys and Implications for the Causes of Plate Motions. *Geophysical Research Letters*, **30,** 2036.

MOUTHEREAU, F., LACOMBE, O., TENSI, J., BELLAHSEN, N., KARGAR, S. & AMROUCH, K. (2007) Mechanical Constraints on the Development of the Zagros Folded Belt (Fars). In: *Thrust Belts and Foreland Basins: From Fold Kinematics to Hydrocarbon Systems: Frontiers in Earth Sciences* (Ed. by O. Lacombe, J. Lavé, F. Roure & J. Verges), 245-264. Springer-Verlag.

MOUTHEREAU, F., TENSI, J., BELLAHSEN, N., LACOMBE, O., DE BOISGROLLIER, T. & KARGAR, S. (2007) Tertiary Sequence of Deformation in a Thin-Skinned/Thick-Skinned Collision Belt: The Zagros Folded Belt (Fars, Iran). *Tectonics*, **26,** TC 5006.

OVEISI, B., LAVE, J., VAN DER BEEK, P., CARCAILLET, J., L., B. & AUBOURG, C. (2009) Thick- and Thin-Skinned Deformation Rates in the Central Zagros Simple Folded Zone (Iran) Indicated by Displacement of Geomorphic Surfaces. *Geophys. J. Int.*, **176,** 627-654.

RAMÍREZ-HERRERA, M.T. (1998) Geomorphic Assessment of Active Tectonics in the Acambay Graben, Mexican Volcanic Belt. *Earth Surface Processes and Landforms*, **23,** 317-332.

RAMSAY, J.G. & HUBER, M.I. (1983) *The Technique of Modern Structural Geology. Vol. 2: Folds and Fractures*. Academic Press, New York.

RAMSEY, L.A., WALKER, R.T. & JACKSON, J. (2008) Fold Evolution and Drainage Development in the Zagros Mountains of Fars Province,Se Iran. *Basin Research*, **20,** 23-48.

SATTARZADEH, Y., COSGROVE, J.W. & VITA-FINZI, C. (2002) The Geometry of Structures in the Zagros Cover Rocks and Its Neotectonic Implications the tectonic and climate Evolution of the Arabian Sea Region. In: *The Tectonic and Climate Evolution of the Arabian Sea Region* (Ed. by P. D. Clift, D. Kroon, C. Gaedicke & J. Craig), **195**, 205-217. The Geological Society of London, Special Publication, London.

SELLA, G.F., DIXON, T.H. & MAO, A. (2002) Revel: A Model for Recent Plate Velocities from Space Geodesy. *J. Geophys. Res.*, **107(B4),** 2081.

SIMPSON, G.D.H. (2006) Modelling Interactions between Fold-Thrust Belt Deformation, Foreland Flexure and Surface Mass Transport. *Basin Research*, **18,** 125-143.

SIMPSON, G.D.H. (2009) Mechanical Modelling of Folding Versus Faulting in Brittle–Ductile Wedges. *Journal of Structural Geology*, **31,** 369-381.

SISSAKIAN, V.K., IBRAHIM, E.I. & AL-WAÌLY, I.J. (1997) Geological Map of Arbeel and Mahabad Quadrangles Sheets Nj-38-14 and Nj-38-15. V. K. Sissakian, State Establishment of Geological Survey and Mining. Baghdad.

STRAHLER, A.N. (1964) Quantitative Geomorphology of Drainage Basins and Channel Networks. In: *Handbook of Applied Hydrology* (Ed. by V. T. Chow), 4-40. McGraw-Hill, New York.

SUPPE, J. (1983) Geometry and Kinematics of Fault-Bend Folding. *American Journal of Science*, **283,** 684-721.

SUPPE, J. & CHANG, Y.-L. (1983) Kink Method Applied to Structural Interpretation of Seismic Sections, Western Taiwan. *Petrol Geol Taiwan*, **19,** 29-49.

TALLING, P.J., HOVIUS, N., STEWART, M.D., KIRKBY, M.J., GUPTA, S., WILKIN, J.C. & STARK, C.P. (1993) Regular Spacing of Drainage Basin Outlets: Implications for Basin Fill Architecture. *British Sedimentological Research Group, Annual meeting*. Manchester.

TALLING, P.J., STEWART, M.D., STARK, C.P., GUPTA, S. & VINCENT, S.J. (1997) Regular Spacing of Drainage Outlets from Linear Fault Blocks. *Basin Research*, **9,** 275-302.

TSODOULOS, I.M., KOUKOUVELAS, I.K. & PAVLIDES, S. (2008) Tectonic Geomorphology of the Easternmost Extension of the Gulf of Corinth (Beotia, Central Greece). *Tectonophysics*, **453,** 211-232.

7. Appendix

All data are separated into data processed by Bernhard Bretis (Permam-,Bana Bawi Anticlines) and Nikolaus Bartl (Safeen Anticlines)

7.1. Abbreviations

Ab	drainage basin area
Ab’	average drainage basin area
W	half width
W’	average half width
S	spacing
S’	average spacing
R	individual drainage basins spacing ratio
R’	average drainage basin spacing ratio
R’’	spacing ratio calculated out of the averages of W and S
Bl	length of the drainage basin
Bl’	average length of the drainage basins
Bw	width of the drainage basin
Bw’	average width of the drainage basins
Bs	individual drainage basins spacing ratio
Bs’	average drainage basin elongation ratio
Bs’’	elongation ratio calculated out of the averages of Bl and Bw
P	perimeter of the drainage basin
P’	average perimeter of the drainage basins
rc	radius of circle with the same perimeter as the drainage basin
Ac	area of the circle
Ac’	average area of the circles
C	individual basins circularity index
C’	average basin circularity index
C’’	circularity index calculated out of the averages of Ab and Ac
Aq	area of the square

Aq’	average area of the squares
Rf	basin shape
Rf’	individual basins basin shape
Rf’’	basin shape calculated out of the averages of Ab and Bl
StDev	standard deviation

The second part of the Appendix is represented by Table 1, which shows an assumption of the average, median and standard deviation values for each measurement and parameter of the quantified segments.

The second part (Table 2) consists of the detailed values for each measurement and parameter of each quantified drainage basin.

7.2. Overview of the statistics (Bartl/Bretis)

Location	Drop (m)	Channel Length (km)	Slope (m/m)	Sinuosity (m/m)	Ab (km^2)	W' (km)	S' (km)	R'	R''	Bl' (km)	Bw' (km)	Bs'	Bs''	P' (km)	C'	C''	Rf'	Rf''
b) Permam																		
Forelimb																		
Average	315	2,494	0,128	1,155	1,025	2,219	0,646	3,701	3,432	2,282	0,524	5,135	4,356	5,595	0,402	0,402	0,193	0,193
Median	314	2,448	0,129	1,132	1,247	2,330	0,577	3,462		2,256	0,544	4,973		5,529	0,402		0,193	
StDev (%)	9%	17%	10%	8%	34%	10%	34%	27%		15%	41%	43%		16%	19%		24%	
Backlimb																		
Average	372	2,892	0,132	1,222	1,307	2,263	0,716	3,201	3,162	2,542	0,658	4,147	3,867	6,306	0,404	0,404	0,199	0,200
Median	367	2,740	0,135	1,182	1,092	2,244	0,722	3,139		2,483	0,559	4,081		6,048	0,412		0,201	
StDev (%)	7%	15%	20%	12%	42%	11%	16%	12%		11%	33%	27%		16%	22%		29%	
c) Bana Bawi NW																		
Forelimb																		
Average	410	3,270	0,130	1,168	1,532	2,658	0,858	3,937	3,097	2,933	0,665	4,596	4,413	7,176	0,377	0,339	0,179	0,164
Median	401	2,904	0,132	1,127	1,327	2,723	0,767	3,067		2,587	0,642	4,014		6,046	0,400		0,176	
StDev (%)	21%	30%	19%	8%	51%	10%	45%	60%		31%	30%	29%		34%	22%		26%	
d) Hogback NW																		
Forelimb																		
Average	289	1,487	0,202	1,145	0,760	1,272	0,801	2,281	1,588	1,430	0,795	2,193	1,799	3,912	0,566	0,561	0,337	0,346
Median	272	1,351	0,203	1,137	0,727	1,127	0,809	1,393		1,268	0,870	2,060		3,773	0,560		0,298	
StDev (%)	31%	36%	7%	3%	65%	29%	48%	88%		31%	53%	50%		38%	8%		36%	
Backlimb																		
Average	276	1,648	0,190	1,132	0,697	1,256	0,599	2,119	2,098	1,430	0,665	2,898	2,150	3,804	0,541	0,572	0,313	0,328
Median	273	1,307	0,177	1,100	0,570	1,229	0,599	2,069		1,301	0,687	1,868		3,469	0,543		0,319	
StDev (%)	11%	43%	19%	5%	65%	16%	12%	19%		21%	52%	68%		26%	28%		39%	
e) Hogback Center																		
Forelimb																		
Average	310	1,443	0,220	1,130	0,583	1,305	0,617	2,449	2,115	1,377	0,535	2,813	2,574	3,603	0,537	0,537	0,295	0,294
Median	311	1,410	0,219	1,100	0,523	1,305	0,570	2,189		1,342	0,494	2,455		3,414	0,532		0,303	
StDev (%)	13%	20%	12%	6%	49%	17%	43%	43%		22%	39%	30%		24%	14%		22%	
Backlimb																		
Average	314	1,757	0,184	1,117	0,823	1,491	0,759	2,119	1,963	1,651	0,605	3,313	2,731	4,371	0,498	0,513	0,284	0,289
Median	300	1,659	0,173	1,115	0,680	1,519	0,730	2,059		1,578	0,593	2,756		4,047	0,516		0,279	
StDev (%)	13%	23%	18%	3%	57%	16%	32%	29%		22%	45%	50%		24%	20%		34%	

Location	Drop (m)	Channel Length (km)	Slope (m/m)	Sinuosity (m/m)	Ab (km^2)	W' (km)	S' (km)	R'	R''	Bl' (km)	Bw' (km)	Bs'	Bs''	P' (km)	C'	C''	Rf'	Rf''
f) Hogback SE																		
Forelimb																		
Average	393	2,326	0,173	1,156	1,454	2,021	0,888	2,456	2,275	2,152	0,864	2,692	2,491	5,750	0,520	0,529	0,302	0,302
Median	387	2,400	0,165	1,128	1,396	2,068	0,864	2,369		2,257	0,879	2,519		5,690	0,524		0,311	
StDev (%)	10%	19%	19%	11%	44%	19%	34%	31%		20%	31%	31%		22%	13%		27%	
f) Hogback SE																		
Backlimb																		
Average	288	1,638	0,181	1,122	0,647	1,405	0,655	2,853	2,146	1,502	0,549	3,545	2,735	4,002	0,454	0,480	0,261	0,278
Median	297	1,551	0,179	1,116	0,480	1,363	0,583	2,283		1,391	0,459	3,104		3,678	0,429		0,251	
StDev (%)	16%	21%	18%	4%	71%	15%	55%	58%		18%	61%	51%		24%	28%		39%	
g) Bana Bawi Core																		
Forelimb																		
Average	275	1,377	0,204	1,106	0,330	1,268	0,419	3,505	3,027	1,299	0,312	4,517	4,158	3,037	0,444	0,415	0,198	0,183
Median	232	1,233	0,207	1,101	0,299	1,103	0,354	2,894		1,105	0,310	4,691		3,071	0,450		0,171	
StDev (%)	36%	29%	15%	4%	48%	25%	49%	41%		27%	34%	33%		30%	23%		41%	
Backlimb																		
Average	380	1,854	0,204	1,162	0,626	1,606	0,645	3,001	2,492	1,591	0,484	3,645	3,286	4,177	0,447	0,444	0,251	0,244
Median	363	1,833	0,203	1,155	0,659	1,622	0,618	2,458		1,538	0,457	3,748		4,246	0,423		0,239	
StDev (%)	19%	14%	18%	5%	28%	12%	43%	50%		13%	36%	32%		13%	17%		28%	
h) Safeen																		
Forlimb																		
Average	640	1,739	0,380	1,113	1,120	1,531	0,987	1,723	1,552	1,662	0,884	2,216	1,880	4,576	0,635	0,638	0,392	0,387
Median	655	1,723	0,363	1,100	0,977	1,580	0,909	1,405		1,639	0,692	1,824		4,613	0,662		0,419	
StDev (%)	13%	25%	18%	2%	53%	18%	33%	45%		23%	49%	49%		25%	12%		28%	
Backlimb																		
Average	683	1,777	0,390	1,094	0,570	1,626	0,470	3,911	3,460	1,713	0,390	5,040	4,389	4,212	0,374	0,383	0,184	0,188
Median	690	1,744	0,376	1,080	0,440	1,705	0,395	3,840		1,705	0,363	4,335		4,084	0,389		0,177	
StDev (%)	21%	22%	17%	4%	63%	22%	50%	32%		19%	39%	43%		24%	25%		36%	
i) Safeen																		
Forlimb																		
Average	442	1,172	0,387	1,076	0,428	1,113	0,521	2,216	2,135	1,096	0,519	2,549	2,113	3,004	0,547	0,569	0,333	0,353
Median	396	1,156	0,413	1,081	0,429	1,116	0,507	2,247		1,113	0,425	2,692		3,017	0,557		0,328	
StDev (%)	22%	9%	15%	2%	52%	9%	24%	20%		10%	47%	45%		23%	16%		38%	
Backlimb																		
Average	486	1,687	0,302	1,084	0,552	1,520	0,608	2,758	2,499	1,513	0,508	3,353	2,976	4,132	0,396	0,403	0,242	0,240
Median	508	1,675	0,305	1,072	0,555	1,540	0,600	2,627		1,477	0,412	4,000		4,088	0,341		0,210	
StDev (%)	29%	5%	23%	3%	39%	4%	37%	31%		8%	41%	33%		10%	30%		41%	

Location	Drop (m)	Channel Length (km)	Slope (m/m)	Sinuosity (m/m)	Ab (km^2)	W' (km)	S' (km)	R'	R''	Bl' (km)	Bw' (km)	Bs'	Bs''	P' (km)	C'	C''	Rf'	Rf''
j) Safeen Forlimb																		
Average	334	1,125	0,305	1,088	0,269	1,078	0,358	3,417	3,013	1,087	0,301	4,475	3,612	2,710	0,430	0,448	0,219	0,224
Median	336	1,124	0,302	1,073	0,254	1,046	0,332	3,354		1,024	0,285	3,614		2,594	0,456		0,216	
StDev (%)	8%	9%	12%	4%	55%	7%	39%	39%		12%	48%	52%		17%	32%		45%	
j) Safeen Backlimb																		
Average	426	1,462	0,292	1,091	0,449	1,404	0,444	3,425	3,166	1,407	0,416	3,964	3,379	3,518	0,424	0,445	0,217	0,225
Median	425	1,479	0,289	1,094	0,497	1,411	0,441	3,200		1,414	0,476	3,097		3,561	0,468		0,243	
StDev (%)	9%	11%	4%	3%	42%	6%	31%	30%		10%	36%	50%		17%	25%		35%	
k) Safeen Forlimb																		
Average	536	1,235	0,444	1,084	0,354	1,213	0,413	3,283	2,935	1,200	0,350	3,792	3,426	3,012	0,481	0,480	0,244	0,244
Median	517	1,259	0,457	1,064	0,355	1,219	0,415	2,677		1,257	0,324	4,071		3,090	0,460		0,228	
StDev (%)	19%	10%	20%	4%	37%	9%	30%	40%		10%	36%	31%		15%	21%		33%	
Backlimb																		
Average	678	1,485	0,466	1,106	0,422	1,325	0,501	2,903	2,645	1,341	0,396	3,858	3,390	3,492	0,422	0,424	0,228	0,232
Median	689	1,512	0,485	1,112	0,401	1,354	0,534	2,401		1,394	0,325	3,725		3,635	0,390		0,208	
StDev (%)	15%	13%	16%	3%	45%	10%	31%	36%		12%	45%	35%		17%	26%		33%	

Table 1: Average, Median and Standard Deviation values for each measurement and parameter of the quantified segment

7.3. Detailed Statistics

7.3.1. Fold segments of Permam-,Bana Bawi Anticlines (Bretis)

b) Permam

Forelimb

Area	Drop	Channel Length	Slope	Sinuosity	Ab	W	S	R	Bl
	(m)	(km)	(m/m)	(m/m)	(km^2)	(km)	(km)		(km)
1	308	2,753	0,112	1,127	1,401	2,353	0,716	3,286	2,542
2	282	2,126	0,133	1,136	0,522	2,311	0,471	4,907	1,898
3	353	2,820	0,125	1,201	1,256	2,422	1,244	1,947	2,805
4	320	2,378	0,135	1,101	1,238	2,161	0,412	5,245	2,190
5	320	2,530	0,126	1,088	0,687	2,349	0,501	4,689	2,264
6	352	2,812	0,125	1,194	1,295	2,424	0,571	4,245	2,418
7	325	2,235	0,145	1,096	0,551	2,456	0,542	4,531	2,008
8	349	3,464	0,101	1,429	1,307	2,387	0,868	2,750	2,850
9	296	2,085	0,142	1,128	0,877	1,861	0,572	3,253	1,914
10	303	2,517	0,120	1,163	1,257	2,113	0,581	3,637	2,247
11	268	1,917	0,140	1,055	0,574	1,785	0,633	2,820	1,847
12	302	2,290	0,132	1,144	1,334	2,004	0,646	3,100	2,403
Average	**315**	**2,494**	**0,128**	**1,155**	**1,025**	**2,219**	**0,646**	**3,701**	**2,282**
Median	**314**	**2,448**	**0,129**	**1,132**	**1,247**	**2,330**	**0,577**	**3,462**	**2,256**
STDEV	**27**	**0,424**	**0,013**	**0,096**	**0,351**	**0,231**	**0,222**	**1,013**	**0,338**
STDEV (%)	**9%**	**17%**	**10%**	**8%**	**34%**	**10%**	**34%**	**27%**	**15%**

R''
3,432

Area	Bw	Bs	P	rc	Ac	C	Aq	Rf
	(km)		(km)	(km)	(km^2)		(km^2)	
1	0,564	4,507	6,552	1,043	3,416	0,410	6,462	0,217
2	0,198	9,586	4,344	0,691	1,502	0,348	3,602	0,145
3	0,401	6,995	6,524	1,038	3,387	0,371	7,868	0,160
4	0,698	3,138	5,497	0,875	2,405	0,515	4,796	0,258
5	0,302	7,497	5,462	0,869	2,374	0,289	5,126	0,134
6	0,656	3,686	6,031	0,960	2,894	0,447	5,847	0,221
7	0,327	6,141	4,787	0,762	1,824	0,302	4,032	0,137
8	0,524	5,439	7,060	1,124	3,966	0,330	8,123	0,161
9	0,823	2,326	4,847	0,771	1,870	0,469	3,663	0,239
10	0,689	3,261	5,560	0,885	2,460	0,511	5,049	0,249
11	0,306	6,036	4,283	0,682	1,460	0,393	3,411	0,168
12	0,799	3,008	6,194	0,986	3,053	0,437	5,774	0,231

Average	**0,524**	**5,135**	**5,595**	**0,890**	**2,551**	**0,402**	**5,313**	**0,193**
Median	**0,544**	**4,973**	**5,529**	**0,880**	**2,432**	**0,402**	**5,087**	**0,193**
STDEV	**0,213**	**2,199**	**0,905**	**0,144**	**0,807**	**0,076**	**1,582**	**0,047**
STDEV (%)	**41%**	**43%**	**16%**	**16%**	**32%**	**19%**	**30%**	**24%**
		Bs''				**C''**		**Rf''**
		4,356				**0,402**		**0,193**

Backlimb

Area	Drop	Channel Length	Slope	Sinuosity	Ab	W	S	R	Bl
	(m)	(km)	(m/m)	(m/m)	(km^2)	(km)	(km)		(km)
1	348	3,425	0,102	1,412	0,932	1,789	0,542	3,301	2,959
2	370	2,780	0,134	1,177	1,200	2,245	0,577	3,891	2,353
3	363	2,680	0,135	1,091	0,927	2,338	0,756	3,093	2,470
4	391	2,610	0,150	1,156	0,984	2,222	0,706	3,147	2,277
5	412	2,347	0,176	1,051	0,807	2,243	0,728	3,081	2,204
6	396	2,700	0,147	1,188	1,316	2,151	0,855	2,516	2,495
7	357	2,961	0,121	1,240	2,042	2,646	0,845	3,131	2,707
8	342	3,635	0,094	1,464	2,245	2,467	0,716	3,448	2,873

Average	**€ 372**	**2,892**	**0,132**	**1,222**	**1,307**	**2,263**	**0,716**	**3,201**	**2,542**
Median	**€ 367**	**2,740**	**0,135**	**1,182**	**1,092**	**2,244**	**0,722**	**3,139**	**2,483**
STDEV	**€ 25**	**0,433**	**0,027**	**0,146**	**0,544**	**0,249**	**0,112**	**0,387**	**0,277**
STDEV (%)	**7%**	**15%**	**20%**	**12%**	**42%**	**11%**	**16%**	**12%**	**11%**
								R''	
								3,162	

Area	Bw	Bs	P	rc	Ac	C	Aq	Rf
	(km)		(km)	(km)	(km^2)		(km^2)	
1	0,527	5,615	6,823	1,086	3,705	0,252	8,756	0,106
2	0,553	4,255	5,695	0,906	2,581	0,465	5,537	0,217
3	0,432	5,718	5,927	0,943	2,796	0,332	6,101	0,152
4	0,506	4,500	5,417	0,862	2,335	0,421	5,185	0,190
5	0,564	3,908	5,212	0,830	2,162	0,373	4,858	0,166
6	0,733	3,404	6,169	0,982	3,028	0,435	6,225	0,211
7	1,042	2,598	6,836	1,088	3,719	0,549	7,328	0,279
8	0,903	3,182	8,369	1,332	5,574	0,403	8,254	0,272

Average	**0,658**	**4,147**	**6,306**	**1,004**	**3,237**	**0,404**	**6,530**	**0,199**
Median	**0,559**	**4,081**	**6,048**	**0,963**	**2,912**	**0,412**	**6,163**	**0,201**
STDEV	**0,215**	**1,115**	**1,023**	**0,163**	**1,105**	**0,089**	**1,436**	**0,059**
STDEV (%)	**33%**	**27%**	**16%**	**16%**	**34%**	**22%**	**22%**	**29%**
		Bs''				**C''**		**Rf''**
		3,867				**0,404**		**0,200**

c) Bana Bawi NW

Forelimb

Area	Drop	Channel Length	Slope	Sinuosity	Ab	W	S	R	Bl
	(m)	(km)	(m/m)	(m/m)	(km^2)	(km)	(km)		(km)
1	383	5,540	0,070	1,411	3,395	2,446	1,216	2,012	5,003
2	299	2,648	0,113	1,151	1,182	2,951	0,615	4,798	2,261
3	308	2,422	0,127	1,112	0,762	2,912	0,312	9,333	2,132
4	332	2,523	0,132	1,126	1,129	2,327	1,426	1,632	2,244
5	440	3,381	0,130	1,221	1,713	2,167	0,758	2,859	3,120
6	509	3,665	0,139	1,187	1,350	2,545	0,883	2,882	3,511
7	544	4,428	0,123	1,203	2,091	2,723	0,693	3,929	3,853
8	345	2,405	0,143	1,106	0,935	2,698	0,381	7,081	2,175
9	401	2,816	0,142	1,107	0,792	2,736	0,892	3,067	2,432
10	417	2,904	0,144	1,127	1,327	2,961	0,767	3,860	2,587
11	533	3,234	0,165	1,096	2,174	2,771	1,497	1,851	2,948
Average	**410**	**3,270**	**0,130**	**1,168**	**1,532**	**2,658**	**0,858**	**3,937**	**2,933**
Median	**401**	**2,904**	**0,132**	**1,127**	**1,327**	**2,723**	**0,767**	**3,067**	**2,587**
STDEV	**88**	**0,970**	**0,024**	**0,091**	**0,780**	**0,260**	**0,386**	**2,370**	**0,895**
STDEV (%)	**21%**	**30%**	**19%**	**8%**	**51%**	**10%**	**45%**	**60%**	**31%**
								R''	
								3,097	

Area	Bw	Bs	P	rc	Ac	C	Aq	Rf
	(km)		(km)	(km)	(km^2)		(km^2)	
1	0,951	5,261	13,097	2,084	13,650	0,249	25,030	0,136
2	0,710	3,185	5,879	0,936	2,750	0,430	5,112	0,231
3	0,543	3,926	4,894	0,779	1,906	0,400	4,545	0,168
4	0,559	4,014	5,731	0,912	2,614	0,432	5,036	0,224
5	0,906	3,444	7,564	1,204	4,553	0,376	9,734	0,176
6	0,523	6,713	7,871	1,253	4,930	0,274	12,327	0,110
7	0,642	6,002	9,524	1,516	7,218	0,290	14,846	0,141
8	0,431	5,046	5,140	0,818	2,102	0,445	4,731	0,198
9	0,387	6,284	5,671	0,903	2,559	0,309	5,915	0,134
10	0,758	3,413	6,046	0,962	2,909	0,456	6,693	0,198
11	0,901	3,272	7,522	1,197	4,503	0,483	8,691	0,250
Average	**0,665**	**4,596**	**7,176**	**1,142**	**4,518**	**0,377**	**9,333**	**0,179**
Median	**0,642**	**4,014**	**6,046**	**0,962**	**2,909**	**0,400**	**6,693**	**0,176**
STDEV	**0,196**	**1,312**	**2,408**	**0,383**	**3,416**	**0,082**	**6,208**	**0,046**
STDEV (%)	**30%**	**29%**	**34%**	**34%**	**76%**	**22%**	**67%**	**26%**
		Bs''				**C''**		**Rf''**
		4,413				**0,339**		**0,164**

d) Hogback NW

Forelimb

Area	Drop	Channel Length	Slope	Sinuosity	Ab	W	S	R	Bl
	(m)	(km)	(m/m)	(m/m)	(km^2)	(km)	(km)		(km)
1	416	2,326	0,179	1,193	1,350	1,911	1,082	1,766	2,130
2	337	1,662	0,203	1,094	1,169	1,263	1,141	1,107	1,568
3	272	1,351	0,201	1,171	0,727	1,127	0,809	1,393	1,268
4	212	1,032	0,206	1,137	0,336	1,008	0,173	5,827	1,133
5	207	1,066	0,221	1,131	0,218	1,051	0,801	1,312	1,051
Average	**289**	**1,487**	**0,202**	**1,145**	**0,760**	**1,272**	**0,801**	**2,281**	**1,430**
Median	**272**	**1,351**	**0,203**	**1,137**	**0,727**	**1,127**	**0,809**	**1,393**	**1,268**
STDEV	**89**	**0,533**	**0,015**	**0,038**	**0,497**	**0,370**	**0,384**	**1,996**	**0,438**
STDEV (%)	**31%**	**36%**	**7%**	**3%**	**65%**	**29%**	**48%**	**88%**	**31%**
								R''	
								1,588	

Area	Bw	Bs	P	rc	Ac	C	Aq	Rf
	(km)		(km)	(km)	(km^2)		(km^2)	
1	0,908	2,346	5,695	0,906	2,581	0,523	4,537	0,298
2	1,382	1,135	5,087	0,810	2,059	0,568	2,459	0,475
3	0,870	1,457	3,773	0,600	1,133	0,642	1,608	0,452
4	0,550	2,060	2,745	0,437	0,600	0,560	1,284	0,262
5	0,265	3,966	2,261	0,360	0,407	0,536	1,105	0,197
Average	**0,795**	**2,193**	**3,912**	**0,623**	**1,356**	**0,566**	**2,198**	**0,337**
Median	**0,870**	**2,060**	**3,773**	**0,600**	**1,133**	**0,560**	**1,608**	**0,298**
STDEV	**0,419**	**1,101**	**1,472**	**0,234**	**0,938**	**0,046**	**1,407**	**0,122**
STDEV (%)	**53%**	**50%**	**38%**	**38%**	**69%**	**8%**	**64%**	**36%**
		Bs''				**C''**		**Rf''**
		1,799				**0,561**		**0,346**

Backlimb

Area	Drop	Channel Length	Slope	Sinuosity	Ab	W	S	R	Bl
	(m)	(km)	(m/m)	(m/m)	(km^2)	(km)	(km)		(km)
1	326	3,204	0,148	1,130	1,557	1,566	0,711	2,203	1,998
2	275	1,653	0,166	1,072	0,570	1,449	0,619	2,341	1,628
3	265	1,648	0,161	1,241	0,977	1,325	0,463	2,862	1,488
4	229	1,296	0,177	1,097	0,512	1,128	0,596	1,893	1,301
5	270	1,296	0,208	1,187	0,625	1,229	0,594	2,069	1,214
6	273	1,129	0,242	1,100	0,126	1,074	0,609	1,764	1,110
7	294	1,307	0,225	1,099	0,515	1,021	0,599	1,705	1,270
Average	**276**	**1,648**	**0,190**	**1,132**	**0,697**	**1,256**	**0,599**	**2,119**	**1,430**
Median	**273**	**1,307**	**0,177**	**1,100**	**0,570**	**1,229**	**0,599**	**2,069**	**1,301**
STDEV	**29**	**0,713**	**0,036**	**0,060**	**0,453**	**0,201**	**0,073**	**0,400**	**0,305**
STDEV (%)	**11%**	**43%**	**19%**	**5%**	**65%**	**16%**	**12%**	**19%**	**21%**
								R''	
								2,098	

Area	Bw	Bs	P	rc	Ac	C	Aq	Rf
	(km)		(km)	(km)	(km^2)		(km^2)	
1	1,230	1,624	5,655	0,900	2,545	0,612	3,992	0,390
2	0,323	5,040	3,975	0,633	1,257	0,453	2,650	0,215
3	0,887	1,678	4,267	0,679	1,449	0,674	2,214	0,441
4	0,687	1,894	3,441	0,548	0,942	0,543	1,693	0,302
5	0,650	1,868	3,324	0,529	0,879	0,711	1,474	0,424
6	0,174	6,379	2,500	0,398	0,497	0,253	1,232	0,102
7	0,705	1,801	3,469	0,552	0,958	0,538	1,613	0,319
Average	**0,665**	**2,898**	**3,804**	**0,605**	**1,218**	**0,541**	**2,124**	**0,313**
Median	**0,687**	**1,868**	**3,469**	**0,552**	**0,958**	**0,543**	**1,693**	**0,319**
STDEV	**0,349**	**1,962**	**0,987**	**0,157**	**0,657**	**0,154**	**0,952**	**0,122**
STDEV (%)	**52%**	**68%**	**26%**	**26%**	**54%**	**28%**	**45%**	**39%**
		Bs''				**C''**		**Rf''**
		2,150				**0,572**		**0,328**

e) Hogback Center

Forelimb

Area	Drop (m)	Channel Length (km)	Slope (m/m)	Sinuosity (m/m)	Ab (km^2)	W (km)	S (km)	R	Bl (km)
1	257	1,052	0,244	1,061	0,353	1,001	0,563	1,778	1,096
2	252	1,077	0,256	1,241	0,255	1,067	0,412	2,590	1,076
3	301	1,250	0,241	1,039	0,373	1,048	0,683	1,534	1,097
4	321	1,309	0,245	1,175	0,470	1,085	0,685	1,584	1,182
5	259	1,316	0,197	1,102	0,515	1,271	0,344	3,695	1,263
6	272	1,351	0,201	1,082	0,551	1,266	0,531	2,384	1,331
7	282	1,044	0,270	1,096	0,210	1,032	0,577	1,789	1,009
8	320	1,468	0,218	1,097	0,463	1,409	0,368	3,829	1,421
9	331	1,651	0,200	1,138	0,814	1,537	1,085	1,417	1,547
10	336	1,950	0,172	1,225	1,201	1,568	0,751	2,088	2,012
11	332	1,503	0,221	1,098	0,376	1,409	0,504	2,796	1,352
12	302	1,656	0,182	1,069	0,585	1,529	0,438	3,491	1,510
13	348	1,504	0,231	1,089	0,835	1,433	1,290	1,111	1,353
14	404	2,019	0,200	1,218	1,100	1,732	0,756	2,291	2,086
15	353	1,636	0,216	1,141	0,704	1,338	0,271	4,937	1,495
16	293	1,304	0,225	1,216	0,530	1,158	0,6172	1,876	1,198
Average	**310**	**1,443**	**0,220**	**1,130**	**0,583**	**1,305**	**0,617**	**2,449**	**1,377**
Median	**311**	**1,410**	**0,219**	**1,100**	**0,523**	**1,305**	**0,570**	**2,189**	**1,342**
STDEV	**41**	**0,291**	**0,027**	**0,065**	**0,283**	**0,225**	**0,267**	**1,055**	**0,310**
STDEV (%)	**13%**	**20%**	**12%**	**6%**	**49%**	**17%**	**43%**	**43%**	**22%**

R''
2,115

Area	Bw (km)	Bs	P (km)	rc (km)	Ac (km^2)	C	Aq (km^2)	Rf
1	0,507	2,162	2,784	0,443	0,617	0,572	1,201	0,294
2	0,264	4,076	2,495	0,397	0,495	0,515	1,158	0,220
3	0,471	2,329	3,179	0,506	0,804	0,464	1,203	0,310
4	0,480	2,463	3,152	0,502	0,791	0,594	1,397	0,336
5	0,492	2,567	3,381	0,538	0,910	0,566	1,595	0,323
6	0,463	2,875	3,430	0,546	0,936	0,589	1,772	0,311
7	0,217	4,650	2,391	0,381	0,455	0,462	1,018	0,206
8	0,34	4,179	3,494	0,556	0,971	0,477	2,019	0,229
9	0,632	2,448	4,166	0,663	1,381	0,589	2,393	0,340
10	0,919	2,189	5,610	0,893	2,504	0,480	4,048	0,297
11	0,405	3,338	3,339	0,531	0,887	0,424	1,828	0,206
12	0,495	3,051	3,854	0,613	1,182	0,495	2,280	0,257
13	0,813	1,664	3,812	0,607	1,156	0,722	1,831	0,456
14	0,935	2,231	5,045	0,803	2,025	0,543	4,351	0,253
15	0,616	2,427	4,125	0,657	1,354	0,520	2,235	0,315
16	0,508	2,358	3,398	0,541	0,919	0,577	1,435	0,369

Average	**0,535**	**2,813**	**3,603**	**0,574**	**1,087**	**0,537**	**1,985**	**0,295**
Median	**0,494**	**2,455**	**3,414**	**0,543**	**0,928**	**0,532**	**1,800**	**0,303**
STDEV	**0,208**	**0,839**	**0,847**	**0,135**	**0,538**	**0,073**	**0,963**	**0,066**
STDEV (%)	**39%**	**30%**	**24%**	**24%**	**49%**	**14%**	**49%**	**22%**
		Bs''				**C''**		**Rf''**
		2,574				**0,537**		**0,294**

Backlimb

Area	Drop (m)	Channel Length (km)	Slope (m/m)	Sinuosity (m/m)	Ab (km^2)	W (km)	S (km)	R	Bl (km)
1	284	1,137	0,250	1,067	0,464	1,024	0,389	2,632	1,096
2	274	1,226	0,223	1,073	0,157	1,211	0,379	3,195	1,076
3	276	1,566	0,176	1,079	0,707	1,362	0,895	1,522	1,097
4	337	2,171	0,155	1,113	1,216	1,695	0,701	2,418	1,182
5	302	2,506	0,121	1,116	1,863	1,885	1,297	1,453	1,263
6	297	1,768	0,168	1,150	0,814	1,541	0,698	2,208	1,331
7	286	1,623	0,170	1,142	0,570	1,497	0,980	1,528	1,009
8	273	1,653	0,165	1,165	1,094	1,241	0,699	1,775	1,421
9	285	1,671	0,171	1,142	0,653	1,291	0,975	1,324	1,547
10	317	1,593	0,199	1,100	0,438	1,554	0,638	2,436	2,012
11	320	1,572	0,204	1,099	0,608	1,425	0,805	1,770	1,352
12	353	1,664	0,212	1,103	0,506	1,665	0,532	3,130	1,510
13	383	1,890	0,203	1,165	0,831	1,689	0,884	1,911	1,353
14	407	2,559	0,159	1,130	1,599	1,793	0,759	2,361	2,086
Average	**314**	**1,757**	**0,184**	**1,117**	**0,823**	**1,491**	**0,759**	**2,119**	**1,377**
Median	**300**	**1,659**	**0,173**	**1,115**	**0,680**	**1,519**	**0,730**	**2,059**	**1,342**
STD	**42**	**0,411**	**0,033**	**0,033**	**0,471**	**0,246**	**0,245**	**0,605**	**0,310**
STDEV (%)	**13%**	**23%**	**18%**	**3%**	**57%**	**16%**	**32%**	**29%**	**22%**
								R''	
								1,963	

Area	Bw (km)	Bs	P (km)	rc (km)	Ac (km^2)	C	Aq (km^2)	Rf
1	0,507	2,162	2,784	0,443	0,617	0,572	1,201	0,294
2	0,264	4,076	2,495	0,397	0,495	0,515	1,158	0,220
3	0,471	2,329	3,179	0,506	0,804	0,464	1,203	0,310
4	0,480	2,463	3,152	0,502	0,791	0,594	1,397	0,336
5	0,492	2,567	3,381	0,538	0,910	0,566	1,595	0,323
6	0,463	2,875	3,430	0,546	0,936	0,589	1,772	0,311
7	0,217	4,650	2,391	0,381	0,455	0,462	1,018	0,206
8	0,34	4,179	3,494	0,556	0,971	0,477	2,019	0,229
9	0,632	2,448	4,166	0,663	1,381	0,589	2,393	0,340
10	0,919	2,189	5,610	0,893	2,504	0,480	4,048	0,297
11	0,405	3,338	3,339	0,531	0,887	0,424	1,828	0,206
12	0,495	3,051	3,854	0,613	1,182	0,495	2,280	0,257
13	0,813	1,664	3,812	0,607	1,156	0,722	1,831	0,456
14	0,935	2,231	5,045	0,803	2,025	0,543	4,351	0,253
Average	**0,535**	**2,813**	**3,603**	**0,574**	**1,087**	**0,537**	**1,985**	**0,295**
Median	**0,494**	**2,455**	**3,414**	**0,543**	**0,928**	**0,532**	**1,800**	**0,303**
STDEV	**0,208**	**0,839**	**0,847**	**0,135**	**0,538**	**0,073**	**0,963**	**0,066**
STDEV (%)	**39%**	**30%**	**24%**	**24%**	**49%**	**14%**	**49%**	**22%**
		Bs''				**C''**		**Rf''**
		2,574				**0,537**		**0,294**

f) Hogback SE

Forelimb

Area	Drop (m)	Channel Length (km)	Slope (m/m)	Sinuosity (m/m)	Ab (km^2)	W (km)	S (km)	R	Bl (km)
1	404	2,181	0,184	1,084	0,927	1,939	0,767	2,528	2,046
2	351	1,675	0,210	1,074	0,448	1,799	0,578	3,112	1,409
3	342	2,030	0,149	1,084	1,169	2,076	0,503	4,127	2,191
4	408	2,925	0,139	1,106	1,991	2,476	1,525	1,624	2,724
5	394	2,722	0,145	1,135	2,405	2,393	1,313	1,823	2,648
6	371	2,484	0,149	1,084	1,292	2,256	0,994	2,270	2,327
7	379	2,819	0,134	1,213	1,984	2,365	1,137	2,080	2,409
8	441	2,677	0,165	1,092	2,228	2,436	0,965	2,524	2,510
9	462	2,787	0,166	1,194	1,892	2,328	0,599	3,886	2,484
10	423	1,705	0,248	1,056	0,892	2,276	1,144	1,990	1,599
11	468	2,713	0,173	1,171	2,237	2,059	0,740	2,782	2,322
12	371	2,316	0,160	1,141	1,499	1,840	0,840	2,190	2,076
13	397	1,836	0,217	1,120	0,402	1,685	0,611	2,758	1,660
14	373	2,653	0,141	1,597	1,767	1,853	1,086	1,706	2,718
15	344	1,869	0,187	1,141	0,921	1,286	0,521	2,468	1,710
16	363	1,826	0,199	1,198	1,217	1,265	0,888	1,424	1,596
Average	**393**	**2,326**	**0,173**	**1,156**	**1,454**	**2,021**	**0,888**	**2,456**	**2,152**
Median	**387**	**2,400**	**0,165**	**1,128**	**1,396**	**2,068**	**0,864**	**2,369**	**2,257**
STDEV	**39**	**0,447**	**0,032**	**0,127**	**0,640**	**0,383**	**0,300**	**0,760**	**0,438**
STDEV (%)	**10%**	**19%**	**19%**	**11%**	**44%**	**19%**	**34%**	**31%**	**20%**

R''
2,275

Area	Bw (km)	Bs	P (km)	rc (km)	Ac (km^2)	C	Aq (km^2)	Rf
1	0,531	3,853	4,871	0,775	1,888	0,491	4,186	0,221
2	0,455	3,097	3,519	0,560	0,985	0,455	1,985	0,226
3	0,690	3,175	5,466	0,870	2,378	0,492	4,800	0,244
4	0,889	3,064	6,967	1,109	3,863	0,515	7,420	0,268
5	1,110	2,386	7,516	1,196	4,495	0,535	7,012	0,343
6	0,823	2,827	5,720	0,910	2,604	0,496	5,415	0,239
7	0,869	2,772	6,847	1,090	3,731	0,532	5,803	0,342
8	0,997	2,518	6,992	1,113	3,890	0,573	6,300	0,354
9	1,017	2,442	6,995	1,113	3,894	0,486	6,170	0,307
10	0,799	2,001	4,290	0,683	1,465	0,609	2,557	0,349
11	1,303	1,782	7,063	1,124	3,970	0,564	5,392	0,415
12	1,039	1,998	5,660	0,901	2,549	0,588	4,310	0,348
13	0,343	4,840	3,851	0,613	1,180	0,341	2,756	0,146
14	1,078	2,521	6,455	1,027	3,316	0,533	7,388	0,239
15	0,701	2,439	4,760	0,758	1,803	0,511	2,924	0,315
16	1,178	1,355	5,030	0,801	2,013	0,604	2,547	0,478

Average	**0,864**	**2,692**	**5,750**	**0,915**	**2,751**	**0,520**	**4,810**	**0,302**
Median	**0,879**	**2,519**	**5,690**	**0,906**	**2,576**	**0,524**	**5,096**	**0,311**
STDEV	**0,269**	**0,832**	**1,270**	**0,202**	**1,134**	**0,066**	**1,838**	**0,083**
STDEV (%)	**31%**	**31%**	**22%**	**22%**	**41%**	**13%**	**38%**	**27%**
		Bs''				**C''**		**Rf''**
		2,491				**0,529**		**0,302**

Backlimb

Area	Drop	Channel Length	Slope	Sinuosity	Ab	W	S	R	Bl
	(m)	(km)	(m/m)	(m/m)	(km^2)	(km)	(km)		(km)
1	317	1,529	0,207	1,104	0,461	1,457	0,301	4,841	1,472
2	368	1,662	0,221	1,082	0,648	1,427	0,508	2,809	1,629
3	334	1,427	0,234	1,103	0,303	1,331	0,583	2,283	1,357
4	343	1,734	0,198	1,087	0,480	1,608	1,603	1,003	1,677
5	314	2,223	0,141	1,183	1,632	1,763	0,373	4,727	1,961
6	335	2,520	0,133	1,156	1,917	1,707	1,122	1,521	2,175
7	320	2,176	0,147	1,152	1,053	1,868	0,805	2,320	1,911
8	287	1,731	0,166	1,166	0,348	1,469	0,922	1,593	1,549
9	297	1,733	0,171	1,083	0,928	1,232	0,688	1,791	1,523
10	300	1,406	0,213	1,116	0,493	1,327	0,299	4,438	1,339
11	292	1,634	0,179	1,128	0,455	1,363	1,148	1,187	1,391
12	285	1,549	0,184	1,177	0,486	1,224	0,284	4,310	1,290
13	300	1,359	0,236	1,064	0,385	1,162	0,161	7,217	1,238
14	199	1,161	0,171	1,073	0,145	1,122	0,526	2,133	1,152
15	203	1,284	0,171	1,160	0,535	1,111	0,551	2,016	1,204
16	232	1,131	0,205	1,053	0,431	1,195	0,744	1,606	1,220
17	243	1,551	0,157	1,186	0,392	1,391	0,724	1,921	1,347
18	252	1,711	0,148	1,163	1,220	1,346	1,062	1,267	1,656
19	279	1,471	0,190	1,108	0,239	1,359	0,415	3,275	1,345
20	300	1,504	0,199	1,060	0,278	1,437	0,277	5,188	1,369
21	244	1,898	0,129	1,158	0,757	1,611	0,655	2,460	1,730
Average	**288**	**1,638**	**0,181**	**1,122**	**0,647**	**1,405**	**0,655**	**2,853**	**1,502**
Median	**297**	**1,551**	**0,179**	**1,116**	**0,480**	**1,363**	**0,583**	**2,283**	**1,391**
STDEV	**45**	**0,344**	**0,032**	**0,044**	**0,462**	**0,209**	**0,361**	**1,649**	**0,273**
STDEV (%)	**16%**	**21%**	**18%**	**4%**	**71%**	**15%**	**55%**	**58%**	**18%**

R''
2,146

Area	Bw	Bs	P	rc	Ac	C	Aq	Rf
	(km)		(km)	(km)	(km^2)		(km^2)	
1	0,364	4,044	3,673	0,585	1,074	0,429	2,167	0,213
2	0,499	3,265	3,930	0,625	1,229	0,527	2,654	0,244
3	0,302	4,493	3,238	0,515	0,834	0,363	1,841	0,165
4	0,488	3,436	4,169	0,664	1,383	0,347	2,812	0,171
5	1,204	1,629	5,651	0,899	2,541	0,642	3,846	0,424
6	1,026	2,120	6,720	1,070	3,594	0,533	4,731	0,405
7	0,767	2,492	5,147	0,819	2,108	0,499	3,652	0,288
8	0,175	8,851	3,936	0,626	1,233	0,282	2,399	0,145
9	1,031	1,477	4,451	0,708	1,577	0,589	2,320	0,400
10	0,454	2,949	3,289	0,523	0,861	0,573	1,793	0,275
11	0,242	5,748	4,088	0,651	1,330	0,342	1,935	0,235
12	0,509	2,534	3,187	0,507	0,808	0,601	1,664	0,292
13	0,459	2,697	3,311	0,527	0,872	0,441	1,533	0,251
14	0,247	4,664	2,710	0,431	0,584	0,248	1,327	0,109
15	0,576	2,090	3,282	0,522	0,857	0,624	1,450	0,369
16	0,393	3,104	3,678	0,585	1,076	0,400	1,488	0,290

17	0,358	3,763	3,416	0,544	0,929	0,422	1,814	0,216
18	1,322	1,253	4,890	0,778	1,903	0,641	2,742	0,445
19	0,236	5,699	3,127	0,498	0,778	0,307	1,809	0,132
20	0,255	5,369	3,380	0,538	0,909	0,306	1,874	0,148
21	0,624	2,772	4,776	0,760	1,815	0,417	2,993	0,253

Average	**0,549**	**3,545**	**4,002**	**0,637**	**1,347**	**0,454**	**2,326**	**0,261**
Median	**0,459**	**3,104**	**3,678**	**0,585**	**1,076**	**0,429**	**1,935**	**0,251**
STDEV	**0,334**	**1,801**	**0,979**	**0,156**	**0,719**	**0,127**	**0,888**	**0,101**
STDEV (%)	**61%**	**51%**	**24%**	**24%**	**53%**	**28%**	**38%**	**39%**
		Bs''				**C''**		**Rf''**
		2,735				**0,480**		**0,278**

g) Bana Bawi Core

Forelimb

Area	Drop	Channel Length	Slope	Sinuosity	Ab	W	S	R	Bl
	(m)	(km)	(m/m)	(m/m)	(km^2)	(km)	(km)		(km)
1	453	1,950	0,232	1,105	0,542	1,745	0,303	5,759	1,820
2	440	1,970	0,223	1,086	0,394	1,781	0,308	5,782	1,804
3	441	2,166	0,204	1,170	0,662	1,843	0,869	2,121	1,965
4	360	1,457	0,247	1,088	0,338	1,658	0,573	2,894	1,349
5	264	1,461	0,181	1,203	0,295	1,263	0,256	4,934	1,463
6	278	1,341	0,207	1,101	0,511	1,241	0,243	5,107	1,243
7	232	1,127	0,206	1,127	0,135	1,103	0,308	3,581	1,105
8	228	1,064	0,214	1,048	0,299	1,057	0,405	2,610	1,058
9	225	1,039	0,217	1,108	0,181	1,009	0,354	2,850	1,023
10	237	1,233	0,204	1,065	0,368	1,053	0,868	1,213	1,007
11	192	1,731	0,111	1,138	0,428	1,175	0,249	4,719	1,597
12	206	1,009	0,204	1,121	0,275	1,005	0,405	2,481	1,016
13	190	1,011	0,214	1,057	0,122	1,001	0,475	2,107	1,005
14	196	1,076	0,182	1,099	0,269	1,070	0,393	2,723	1,008
15	185	1,027	0,210	1,070	0,128	1,015	0,275	3,691	1,020
Average	**275**	**1,377**	**0,204**	**1,106**	**0,330**	**1,268**	**0,419**	**3,505**	**1,299**
Median	**232**	**1,233**	**0,207**	**1,101**	**0,299**	**1,103**	**0,354**	**2,894**	**1,105**
STDEV	**98**	**0,398**	**0,031**	**0,042**	**0,160**	**0,318**	**0,204**	**1,434**	**0,346**
STDEV (%)	**36%**	**29%**	**15%**	**4%**	**48%**	**25%**	**49%**	**41%**	**27%**
								R''	
								3,027	

Area	Bw	Bs	P	rc	Ac	C	Aq	Rf
	(km)		(km)	(km)	(km^2)		(km^2)	
1	0,388	4,691	4,440	0,707	1,569	0,345	3,312	0,164
2	0,262	6,885	4,120	0,656	1,351	0,292	3,254	0,121
3	0,399	4,925	4,607	0,733	1,689	0,392	3,861	0,171
4	0,318	4,242	3,071	0,489	0,750	0,450	1,820	0,186
5	0,235	6,226	3,346	0,533	0,891	0,331	2,140	0,138
6	0,541	2,298	3,194	0,508	0,812	0,629	1,545	0,331
7	0,180	6,139	2,091	0,333	0,348	0,388	1,221	0,111
8	0,265	3,992	2,720	0,433	0,589	0,508	1,119	0,267
9	0,327	3,128	2,098	0,334	0,350	0,517	1,047	0,173
10	0,413	2,438	3,119	0,496	0,774	0,475	1,014	0,363
11	0,310	5,152	3,939	0,627	1,235	0,347	2,550	0,168
12	0,424	2,396	2,360	0,376	0,443	0,620	1,032	0,266
13	0,182	5,522	2,067	0,329	0,340	0,359	1,010	0,121
14	0,273	3,692	2,575	0,410	0,528	0,510	1,016	0,265
15	0,169	6,036	1,813	0,289	0,262	0,489	1,040	0,123

Average	**0,312**	**4,517**	**3,037**	**0,483**	**0,795**	**0,444**	**1,799**	**0,198**
Median	**0,310**	**4,691**	**3,071**	**0,489**	**0,750**	**0,450**	**1,221**	**0,171**
STDEV	**0,105**	**1,507**	**0,908**	**0,144**	**0,466**	**0,104**	**0,992**	**0,081**
STDEV (%)	**34%**	**33%**	**30%**	**30%**	**59%**	**23%**	**55%**	**41%**
		Bs''				**C''**		**Rf''**
		4,158				**0,415**		**0,183**

Backlimb

Area	Drop (m)	Channel Length (km)	Slope (m/m)	Sinuosity (m/m)	Ab (km^2)	W (km)	S (km)	R	Bl (km)
1	348	1,411	0,203	1,092	0,444	1,208	0,828	1,459	1,270
2	423	1,991	0,212	1,194	0,840	1,717	0,409	4,198	1,538
3	415	1,901	0,218	1,165	0,499	1,667	0,994	1,677	1,444
4	463	1,693	0,274	1,062	0,696	1,664	0,499	3,335	1,460
5	486	2,013	0,241	1,120	0,636	1,622	0,761	2,131	1,665
6	498	2,201	0,226	1,186	0,784	1,704	0,618	2,757	1,904
7	447	1,833	0,244	1,155	0,889	1,611	0,995	1,619	1,599
8	378	1,532	0,235	1,167	0,719	1,963	1,180	1,664	1,657
9	302	1,611	0,187	1,118	0,330	1,455	0,592	2,458	1,433
10	291	1,816	0,160	1,314	0,659	1,498	0,371	4,038	1,358
11	297	2,028	0,146	1,142	0,805	1,797	0,422	4,258	1,819
12	338	2,309	0,146	1,253	0,715	1,757	0,250	7,028	1,775
13	339	1,698	0,200	1,135	0,432	1,599	0,773	2,069	1,502
14	363	2,079	0,175	1,145	0,501	1,319	0,331	3,985	1,946
15	315	1,694	0,186	1,190	0,438	1,506	0,645	2,337	1,491
Average	**380**	**1,854**	**0,204**	**1,162**	**0,626**	**1,606**	**0,645**	**3,001**	**1,591**
Median	**363**	**1,833**	**0,203**	**1,155**	**0,659**	**1,622**	**0,618**	**2,458**	**1,538**
STDEV	**70**	**0,252**	**0,037**	**0,062**	**0,173**	**0,189**	**0,274**	**1,503**	**0,200**
STDEV (%)	**19%**	**14%**	**18%**	**5%**	**28%**	**12%**	**43%**	**50%**	**13%**
								R''	
								2,492	

Area	Bw (km)	Bs	P (km)	rc (km)	Ac (km^2)	C	Aq (km^2)	Rf
1	0,401	3,167	3,127	0,498	0,778	0,571	1,613	0,275
2	0,865	1,778	4,691	0,747	1,751	0,480	2,365	0,355
3	0,320	4,513	4,246	0,676	1,435	0,348	2,085	0,239
4	0,549	2,659	4,173	0,664	1,386	0,502	2,132	0,327
5	0,346	4,812	4,575	0,728	1,666	0,382	2,772	0,229
6	0,508	3,748	4,843	0,771	1,866	0,420	3,625	0,216
7	0,765	2,090	4,578	0,729	1,668	0,533	2,557	0,348
8	0,579	2,862	4,136	0,658	1,361	0,528	2,746	0,262
9	0,265	5,408	3,282	0,522	0,857	0,385	2,053	0,161
10	0,653	2,080	3,872	0,616	1,193	0,552	1,844	0,357
11	0,457	3,980	4,889	0,778	1,902	0,423	3,309	0,243
12	0,497	3,571	4,584	0,730	1,672	0,428	3,151	0,227
13	0,337	4,457	3,674	0,585	1,074	0,402	2,256	0,191
14	0,362	5,376	4,299	0,684	1,471	0,341	3,787	0,132
15	0,357	4,176	3,681	0,586	1,078	0,406	2,223	0,197
Average	**0,484**	**3,645**	**4,177**	**0,665**	**1,411**	**0,447**	**2,568**	**0,251**
Median	**0,457**	**3,748**	**4,246**	**0,676**	**1,435**	**0,423**	**2,365**	**0,239**
STDEV	**0,173**	**1,179**	**0,549**	**0,087**	**0,353**	**0,075**	**0,652**	**0,070**
STDEV (%)	**36%**	**32%**	**13%**	**13%**	**25%**	**17%**	**25%**	**28%**
		Bs''				**C''**		**Rf''**
		3,286				**0,444**		**0,244**

7.3.2. Fold segments of Safeen Anticline (Bartl)

h) Safeen

Forelimb

Area	Drop	Channel Length	Slope	Sinuosity	Ab	W	S	R	Bl
	(m)	(km)	(m/m)	(m/m)	(km^2)	(km)	(km)		(km)
1	660	1,329	0,497	1,148	0,735	1,191	0,907	1,313	1,320
2	741	1,983	0,374	1,097	1,734	1,784	1,638	1,089	1,885
3	754	2,379	0,317	1,092	2,214	1,827	0,541	3,377	2,211
4	650	2,180	0,298	1,151	0,985	1,695	0,794	2,135	2,098
5	664	1,885	0,352	1,117	0,968	1,782	0,876	2,034	1,751
6	533	1,561	0,341	1,096	1,255	1,465	1,240	1,181	1,527
7	589	1,371	0,430	1,097	0,501	1,362	0,910	1,497	1,335
8	525	1,224	0,429	1,103	0,570	1,144	0,987	1,160	1,170
Average	**640**	**1,739**	**0,380**	**1,113**	**1,120**	**1,531**	**0,987**	**1,723**	**1,662**
Median	**655**	**1,723**	**0,363**	**1,100**	**0,977**	**1,580**	**0,909**	**1,405**	**1,639**
STDEV	**86**	**0,428**	**0,067**	**0,024**	**0,594**	**0,278**	**0,327**	**0,778**	**0,384**
STDEV (%)	**13%**	**25%**	**18%**	**2%**	**53%**	**151%**	**96%**	**45%**	**23%**
								R''	
								1,552	

Area	Bw	Bs	P	rc	Ac	C	Aq	Rf
	(km)		(km)	(km)	(km^2)		(km^2)	
1	0,731	1,806	3,763	0,599	1,127	0,652	1,742	0,422
2	1,294	1,457	5,677	0,904	2,565	0,676	3,553	0,488
3	1,675	1,320	6,440	1,025	3,300	0,671	4,889	0,453
4	0,464	4,522	4,967	0,791	1,963	0,502	4,402	0,224
5	0,652	2,686	4,466	0,711	1,587	0,610	3,066	0,316
6	1,136	1,344	4,760	0,758	1,803	0,696	2,332	0,538
7	0,485	2,753	3,406	0,542	0,923	0,543	1,782	0,281
8	0,635	1,843	3,127	0,498	0,778	0,733	1,369	0,416
Average	**0,884**	**2,216**	**4,576**	**0,728**	**1,756**	**0,635**	**2,892**	**0,392**
Median	**0,692**	**1,824**	**4,613**	**0,734**	**1,695**	**0,662**	**2,699**	**0,419**
STDEV	**0,436**	**1,087**	**1,135**	**0,181**	**0,858**	**0,079**	**1,305**	**0,108**
STDEV (%)	**49%**	**49%**	**25%**	**25%**	**49%**	**12%**	**45%**	**28%**
		Bs''				**C''**		**Rf''**
		1,880				**0,638**		**0,387**

Backlimb

Area	Drop	Channel Length	Slope	Sinuosity	Ab	W	S	R	Bl
	(m)	(km)	(m/m)	(m/m)	(km^2)	(km)	(km)		(km)
1	374	1,132	0,330	1,073	0,403	1,010	0,285	3,544	1,281
2	425	1,335	0,318	1,045	0,250	1,075	0,528	2,036	1,183
3	388	0,939	0,413	1,075	0,245	1,103	0,232	4,754	1,189
4	545	1,728	0,315	1,126	0,302	1,222	0,279	4,380	1,963
5	550	1,579	0,348	1,118	0,239	1,189	0,355	3,349	1,452
6	568	1,471	0,386	1,082	0,333	1,327	0,469	2,829	1,377
7	643	1,868	0,344	1,261	0,327	1,342	0,285	4,709	1,905
8	612	1,394	0,439	1,092	0,348	1,477	0,639	2,311	1,317
9	644	1,353	0,477	1,069	0,406	1,415	0,388	3,647	1,342
10	672	1,541	0,436	1,131	0,176	1,451	0,284	5,109	1,454
11	735	1,588	0,463	1,075	0,651	1,480	0,361	4,100	1,614
12	792	1,703	0,465	1,074	0,431	1,579	0,409	3,861	1,671
13	810	1,795	0,451	1,052	0,412	1,710	0,446	3,834	1,772
14	815	1,700	0,479	1,045	0,448	1,704	0,389	4,380	1,560
15	823	1,677	0,491	1,014	0,255	1,705	0,400	4,263	1,711
16	889	1,942	0,458	1,062	0,584	1,900	0,520	3,654	1,905
17	876	2,005	0,437	1,121	0,696	1,939	0,544	3,564	1,864
18	804	1,760	0,457	1,078	0,734	1,913	0,557	3,434	1,698
19	816	2,235	0,365	1,103	1,468	2,134	1,107	1,928	2,163
20	692	1,980	0,349	1,077	0,519	1,718	0,307	5,596	1,808
21	687	2,218	0,310	1,138	1,082	1,885	0,809	2,330	1,885
22	789	2,267	0,348	1,073	0,617	2,269	1,179	1,925	2,172
23	782	2,676	0,292	1,108	1,511	2,122	0,309	6,867	2,371
24	694	2,233	0,311	1,109	0,687	1,933	0,357	5,415	2,084
25	674	1,953	0,345	1,096	0,623	1,870	0,311	6,013	1,660
26	658	2,136	0,308	1,145	1,072	1,807	0,470	3,845	2,133
Average	**683**	**1,777**	**0,390**	**1,094**	**0,570**	**1,626**	**0,470**	**3,911**	**1,713**
Median	**690**	**1,744**	**0,376**	**1,080**	**0,440**	**1,705**	**0,395**	**3,840**	**1,705**
STDEV	**143**	**0,392**	**0,066**	**0,046**	**0,358**	**0,350**	**0,237**	**1,268**	**0,328**
STDEV (%)	**21%**	**22%**	**17%**	**4%**	**63%**	**22%**	**50%**	**32%**	**19%**

R''
3,460

Area	Bw	Bs	P	rc	Ac	C	Aq	Rf
	(km)		(km)	(km)	(km^2)		(km^2)	
1	0,471	2,720	3,179	0,506	0,804	0,501	1,641	0,246
2	0,212	5,580	2,794	0,445	0,621	0,402	1,399	0,179
3	0,281	4,231	2,780	0,442	0,615	0,398	1,414	0,173
4	0,293	6,700	4,406	0,701	1,545	0,195	3,853	0,078
5	0,278	5,223	3,133	0,499	0,781	0,306	2,108	0,113
6	0,294	4,684	3,077	0,490	0,753	0,442	1,896	0,176
7	0,195	9,769	4,127	0,657	1,355	0,241	3,629	0,090
8	0,361	3,648	3,349	0,533	0,893	0,390	1,734	0,201
9	0,364	3,687	3,473	0,553	0,960	0,423	1,801	0,225
10	0,143	10,168	3,089	0,492	0,759	0,232	2,114	0,083
11	0,545	2,961	3,958	0,630	1,247	0,522	2,605	0,250

12	0,259	6,452	3,820	0,608	1,161	0,371	2,792	0,154
13	0,294	6,027	4,025	0,641	1,289	0,320	3,140	0,131
14	0,388	4,021	4,040	0,643	1,299	0,345	2,434	0,184
15	0,169	10,124	3,790	0,603	1,143	0,223	2,928	0,087
16	0,333	5,721	4,354	0,693	1,509	0,387	3,629	0,161
17	0,420	4,438	4,640	0,738	1,713	0,406	3,474	0,200
18	0,527	3,222	4,940	0,786	1,942	0,378	2,883	0,255
19	0,709	3,051	5,749	0,915	2,630	0,558	4,679	0,314
20	0,473	3,822	4,454	0,709	1,579	0,329	3,269	0,159
21	0,569	3,313	5,402	0,860	2,322	0,466	3,553	0,305
22	0,353	6,153	5,000	0,796	1,989	0,310	4,718	0,131
23	0,604	3,925	6,567	1,045	3,432	0,440	5,622	0,269
24	0,405	5,146	5,320	0,847	2,252	0,305	4,343	0,158
25	0,566	2,933	4,343	0,691	1,501	0,415	2,756	0,226
26	0,640	3,333	5,695	0,906	2,581	0,415	4,550	0,236

Average	**0,390**	**5,040**	**4,212**	**0,670**	**1,488**	**0,374**	**3,037**	**0,184**
Median	**0,363**	**4,335**	**4,084**	**0,650**	**1,327**	**0,389**	**2,905**	**0,177**
STDEV	**0,153**	**2,175**	**0,996**	**0,159**	**0,711**	**0,092**	**1,137**	**0,067**
STDEV (%)	**39%**	**43%**	**24%**	**24%**	**48%**	**25%**	**37%**	**36%**
		Bs''				**C''**		**Rf''**
		4,389				**0,383**		**0,188**

i) Safeen

Forelimb

Area	Drop (m)	Channel Length (km)	Slope (m/m)	Sinuosity (m/m)	Ab (km^2)	W (km)	S (km)	R	Bl (km)
1	515	1,232	0,432	1,097	0,694	1,201	0,426	2,819	1,210
2	517	1,189	0,435	1,081	0,333	1,166	0,519	2,247	1,112
3	587	1,364	0,430	1,081	0,717	1,251	0,507	2,467	1,188
4	382	1,103	0,413	1,056	0,112	1,033	0,476	2,170	0,869
5	396	1,156	0,299	1,096	0,429	1,116	0,786	1,420	1,144
6	370	1,073	0,315	1,058	0,448	1,015	0,414	2,452	1,113
7	328	1,088	0,385	1,062	0,261	1,008	0,521	1,934	1,037
Average	**442**	**1,172**	**0,387**	**1,076**	**0,428**	**1,113**	**0,521**	**2,216**	**1,096**
Median	**396**	**1,156**	**0,413**	**1,081**	**0,429**	**1,116**	**0,507**	**2,247**	**1,113**
STDEV	**97**	**0,102**	**0,058**	**0,017**	**0,220**	**0,097**	**0,124**	**0,447**	**0,115**
STDEV (%)	**22%**	**9%**	**15%**	**2%**	**52%**	**9%**	**24%**	**20%**	**10%**
								R''	
								2,135	

Area	Bw (km)	Bs	P (km)	rc (km)	Ac (km^2)	C	Aq (km^2)	Rf
1	0,832	1,454	3,674	0,585	1,074	0,646	1,464	0,474
2	0,378	2,942	2,830	0,450	0,637	0,522	1,237	0,269
3	0,790	1,504	3,971	0,632	1,255	0,571	1,411	0,508
4	0,186	4,672	1,940	0,309	0,299	0,374	0,755	0,148
5	0,425	2,692	3,169	0,504	0,799	0,537	1,309	0,328
6	0,662	1,681	3,017	0,480	0,724	0,618	1,239	0,362
7	0,358	2,897	2,427	0,386	0,469	0,557	1,075	0,243
Average	**0,519**	**2,549**	**3,004**	**0,478**	**0,751**	**0,547**	**1,213**	**0,333**
Median	**0,425**	**2,692**	**3,017**	**0,480**	**0,724**	**0,557**	**1,239**	**0,328**
STDEV	**0,244**	**1,144**	**0,696**	**0,111**	**0,331**	**0,088**	**0,239**	**0,128**
STDEV (%)	**47%**	**45%**	**23%**	**23%**	**44%**	**16%**	**20%**	**38%**
		Bs''				**C''**		**Rf''**
		2,113				**0,569**		**0,353**

Backlimb

Area	Drop	Channel Length	Slope	Sinuosity	Ab	W	S	R	Bl
	(m)	(km)	(m/m)	(m/m)	(km^2)	(km)	(km)		(km)
1	588	1,675	0,351	1,066	0,588	1,58	0,433	3,649	1,665
2	641	1,748	0,367	1,055	0,353	1,54	0,472	3,263	1,539
3	627	1,603	0,391	1,048	0,310	1,457	0,653	2,231	1,396
4	508	1,664	0,305	1,142	0,811	1,451	1,077	1,347	1,474
5	365	1,576	0,232	1,094	0,854	1,447	0,6	2,412	1,477
6	389	1,836	0,212	1,114	0,555	1,568	0,415	3,778	1,667
7	285	1,706	0,258	1,072	0,395	1,598	0,608	2,627	1,372
Average	**486**	**1,687**	**0,302**	**1,084**	**0,552**	**1,520**	**0,608**	**2,758**	**1,513**
Median	**508**	**1,675**	**0,305**	**1,072**	**0,555**	**1,540**	**0,600**	**2,627**	**1,477**
STDEV	**141**	**0,088**	**0,070**	**0,034**	**0,217**	**0,066**	**0,227**	**0,865**	**0,118**
STDEV (%)	**29%**	**5%**	**23%**	**3%**	**39%**	**4%**	**37%**	**31%**	**8%**
								R''	
								2,499	

Area	Bw	Bs	P	rc	Ac	C	Aq	Rf
	(km)		(km)	(km)	(km^2)		(km^2)	
1	0,412	4,041	4,710	0,750	1,765	0,333	2,772	0,212
2	0,345	4,461	3,760	0,598	1,125	0,314	2,369	0,149
3	0,349	4,000	3,643	0,580	1,056	0,294	1,949	0,159
4	0,791	1,863	4,088	0,651	1,330	0,610	2,173	0,373
5	0,824	1,792	4,600	0,732	1,684	0,507	2,182	0,391
6	0,398	4,188	4,312	0,686	1,480	0,375	2,779	0,200
7	0,439	3,125	3,813	0,607	1,157	0,341	1,882	0,210
Average	**0,508**	**3,353**	**4,132**	**0,658**	**1,371**	**0,396**	**2,301**	**0,242**
Median	**0,412**	**4,000**	**4,088**	**0,651**	**1,330**	**0,341**	**2,182**	**0,210**
STDEV	**0,207**	**1,120**	**0,422**	**0,067**	**0,281**	**0,117**	**0,362**	**0,099**
STDEV (%)	**41%**	**33%**	**10%**	**10%**	**20%**	**30%**	**16%**	**41%**
		Bs''				**C''**		**Rf''**
		2,976				**0,403**		**0,240**

j) Safeen

Forelimb

Area	Drop	Channel Length	Slope	Sinuosity	Ab	W	S	R	Bl
	(m)	(km)	(m/m)	(m/m)	(km^2)	(km)	(km)		(km)
1	337	1,124	0,300	1,132	0,297	1,144	0,312	3,667	1,143
2	315	1,184	0,266	1,075	0,248	1,147	0,279	4,111	1,169
3	294	0,944	0,312	1,059	0,194	1,150	0,332	3,464	0,946
4	343	1,176	0,292	1,094	0,343	1,108	0,426	2,601	1,124
5	316	1,149	0,275	1,069	0,561	1,088	0,567	1,919	1,110
6	368	1,131	0,325	1,059	0,179	1,017	0,318	3,198	1,024
7	363	1,214	0,299	1,141	0,099	1,015	0,213	4,765	1,021
8	359	1,130	0,318	1,064	0,286	1,043	0,355	2,938	1,067
9	336	1,111	0,302	1,122	0,116	1,020	0,345	2,957	1,023
10	313	1,047	0,321	1,034	0,166	1,054	0,362	2,912	0,948
11	323	1,139	0,327	1,100	0,309	1,018	0,351	2,900	1,385
12	327	1,095	0,327	1,073	0,276	1,002	0,480	2,088	1,019
13	331	1,099	0,301	1,177	0,428	1,009	0,286	3,528	1,022
14	338	1,026	0,329	1,090	0,254	1,004	0,432	2,324	1,041
15	349	1,416	0,246	1,216	0,622	1,017	0,822	1,237	1,402
16	373	1,041	0,358	1,019	0,091	1,150	0,144	7,986	1,013
17	370	1,077	0,377	1,025	0,075	1,030	0,242	4,256	0,987
18	374	1,029	0,364	1,071	0,201	1,046	0,302	3,464	1,010
19	309	1,189	0,260	1,068	0,455	1,203	0,287	4,192	1,215
20	265	1,056	0,251	1,100	0,185	1,173	0,301	3,897	0,911
21	319	1,246	0,256	1,063	0,256	1,200	0,358	3,352	1,257
Average	**334**	**1,125**	**0,305**	**1,088**	**0,269**	**1,078**	**0,358**	**3,417**	**1,087**
Median	**336**	**1,124**	**0,302**	**1,073**	**0,254**	**1,046**	**0,332**	**3,352**	**1,024**
STDEV	**28**	**0,098**	**0,037**	**0,048**	**0,148**	**0,071**	**0,140**	**1,350**	**0,134**
STDEV (%)	**8%**	**9%**	**12%**	**4%**	**55%**	**7%**	**39%**	**39%**	**12%**

R''
3,013

Area	Bw	Bs	P	rc	Ac	C	Aq	Rf
	(km)		(km)	(km)	(km^2)		(km^2)	
1	0,327	3,495	2,812	0,448	0,629	0,472	1,306	0,227
2	0,253	4,621	2,972	0,473	0,703	0,352	1,367	0,181
3	0,266	3,556	2,173	0,346	0,376	0,515	0,895	0,216
4	0,311	3,614	2,979	0,474	0,706	0,486	1,263	0,271
5	0,671	1,654	3,112	0,495	0,771	0,728	1,232	0,455
6	0,230	4,452	2,626	0,418	0,549	0,326	1,049	0,171
7	0,134	7,619	2,544	0,405	0,515	0,192	1,042	0,095
8	0,285	3,744	2,594	0,413	0,535	0,534	1,138	0,251
9	0,138	7,413	2,297	0,366	0,420	0,276	1,047	0,111
10	0,196	4,837	2,227	0,354	0,395	0,421	0,899	0,185
11	0,379	3,654	3,194	0,508	0,812	0,381	1,918	0,161
12	0,404	2,522	2,512	0,400	0,502	0,550	1,038	0,266

13	0,482	2,120	3,024	0,481	0,728	0,588	1,044	0,410
14	0,331	3,145	2,579	0,410	0,529	0,480	1,084	0,234
15	0,515	2,722	3,908	0,622	1,215	0,512	1,966	0,316
16	0,149	6,799	2,287	0,364	0,416	0,219	1,026	0,089
17	0,086	11,477	2,101	0,334	0,351	0,214	0,974	0,077
18	0,295	3,424	2,382	0,379	0,452	0,445	1,020	0,197
19	0,430	2,826	3,201	0,509	0,815	0,558	1,476	0,308
20	0,253	3,601	2,258	0,359	0,406	0,456	0,830	0,223
21	0,188	6,686	3,124	0,497	0,777	0,330	1,580	0,162

Average	**0,301**	**4,475**	**2,710**	**0,431**	**0,600**	**0,430**	**1,200**	**0,219**
Median	**0,285**	**3,614**	**2,594**	**0,413**	**0,535**	**0,456**	**1,049**	**0,216**
STDEV	**0,143**	**2,329**	**0,456**	**0,073**	**0,210**	**0,138**	**0,311**	**0,098**
STDEV (%)	**48%**	**52%**	**17%**	**17%**	**35%**	**32%**	**26%**	**45%**
		Bs''				**C''**		**Rf''**
		3,612				**0,448**		**0,224**

Backlimb

Area	Drop	Channel Length	Slope	Sinuosity	Ab	W	S	R	Bl
	(m)	(km)	(m/m)	(m/m)	(km^2)	(km)	(km)		(km)
1	425	1,473	0,288	1,118	0,374	1,331	0,243	5,477	1,414
2	434	1,566	0,277	1,132	0,497	1,418	0,552	2,569	1,324
3	421	1,479	0,285	1,124	0,240	1,290	0,345	3,739	1,299
4	416	1,438	0,289	1,094	0,508	1,360	0,487	2,793	1,394
5	422	1,481	0,285	1,068	0,491	1,411	0,441	3,200	1,444
6	481	1,653	0,291	1,123	0,627	1,512	0,418	3,617	1,526
7	336	1,066	0,315	1,023	0,081	1,478	0,339	4,360	1,177
8	451	1,533	0,294	1,076	0,665	1,523	0,723	2,107	1,654
9	451	1,468	0,307	1,063	0,562	1,314	0,444	2,963	1,431
Average	**426**	**1,462**	**0,292**	**1,091**	**0,449**	**1,404**	**0,444**	**3,425**	**1,407**
Median	**425**	**1,479**	**0,289**	**1,094**	**0,497**	**1,411**	**0,441**	**3,200**	**1,414**
STDEV	**40**	**0,162**	**0,012**	**0,036**	**0,188**	**0,087**	**0,138**	**1,022**	**0,136**
STDEV (%)	**9%**	**11%**	**4%**	**3%**	**42%**	**6%**	**31%**	**30%**	**10%**
								R''	
								3,166	

Area	Bw	Bs	P	rc	Ac	C	Aq	Rf
	(km)		(km)	(km)	(km^2)		(km^2)	
1	0,285	4,961	3,431	0,546	0,937	0,399	1,999	0,187
2	0,429	3,086	3,653	0,581	1,062	0,468	1,753	0,284
3	0,298	4,359	3,209	0,511	0,819	0,293	1,687	0,142
4	0,476	2,929	3,481	0,554	0,964	0,527	1,943	0,261
5	0,494	2,923	3,561	0,567	1,009	0,487	2,085	0,235
6	0,487	3,133	4,010	0,638	1,280	0,490	2,329	0,269
7	0,133	8,850	2,227	0,354	0,395	0,205	1,385	0,058
8	0,534	3,097	4,332	0,689	1,493	0,445	2,736	0,243
9	0,612	2,338	3,756	0,598	1,123	0,501	2,048	0,274
Average	**0,416**	**3,964**	**3,518**	**0,560**	**1,009**	**0,424**	**1,996**	**0,217**
Median	**0,476**	**3,097**	**3,561**	**0,567**	**1,009**	**0,468**	**1,999**	**0,243**
STDEV	**0,149**	**2,001**	**0,587**	**0,093**	**0,305**	**0,108**	**0,387**	**0,075**
STDEV (%)	**36%**	**50%**	**17%**	**17%**	**30%**	**25%**	**19%**	**35%**
		Bs''				**C''**		**Rf''**
		3,379				**0,445**		**0,225**

k) Safeen

Forelimb

Area	Drop (m)	Channel Length (km)	Slope (m/m)	Sinuosity (m/m)	Ab (km^2)	W (km)	S (km)	R	Bl (km)
1	354	1,239	0,286	1,119	0,596	1,193	0,305	3,911	1,237
2	345	1,044	0,330	1,137	0,159	1,114	0,190	5,863	0,971
3	476	1,356	0,351	1,108	0,407	1,125	0,527	2,135	1,271
4	484	1,234	0,473	1,026	0,353	1,111	0,544	2,042	1,018
5	499	1,389	0,359	1,128	0,375	1,286	0,226	5,690	1,271
6	498	1,069	0,466	1,060	0,193	1,083	0,399	2,714	1,078
7	524	1,036	0,560	1,069	0,341	1,006	0,393	2,560	1,021
8	619	1,101	0,562	1,054	0,242	1,072	0,416	2,577	1,108
9	623	1,196	0,538	1,057	0,227	1,232	0,400	3,080	1,180
10	663	1,309	0,507	1,082	0,401	1,244	0,571	2,179	1,380
11	450	1,279	0,352	1,138	0,421	1,270	0,481	2,640	1,270
12	673	1,161	0,580	1,040	0,356	1,398	0,576	2,427	1,256
13	704	1,401	0,503	1,121	0,690	1,206	0,477	2,528	1,257
14	504	1,096	0,460	1,052	0,271	1,147	0,565	2,030	1,113
15	520	1,314	0,396	1,152	0,400	1,301	0,222	5,860	1,285
16	586	1,353	0,433	1,056	0,399	1,375	0,305	4,508	1,316
17	514	1,318	0,390	1,056	0,276	1,345	0,426	3,157	1,273
18	606	1,336	0,454	1,049	0,267	1,318	0,413	3,190	1,295
Average	**536**	**1,235**	**0,444**	**1,084**	**0,354**	**1,213**	**0,413**	**3,283**	**1,200**
Median	**517**	**1,259**	**0,457**	**1,064**	**0,355**	**1,219**	**0,415**	**2,677**	**1,257**
STDEV	**101**	**0,123**	**0,088**	**0,040**	**0,133**	**0,113**	**0,123**	**1,323**	**0,119**
STDEV (%)	**19%**	**10%**	**20%**	**4%**	**37%**	**9%**	**30%**	**40%**	**10%**

R''
2,935

Area	Bw (km)	Bs	P (km)	rc (km)	Ac (km^2)	C	Aq (km^2)	Rf
1	0,605	2,045	3,307	0,526	0,870	0,685	1,530	0,389
2	0,212	4,580	2,078	0,331	0,344	0,463	0,943	0,169
3	0,460	2,763	3,152	0,502	0,791	0,515	1,615	0,252
4	0,417	2,441	2,629	0,418	0,550	0,642	1,036	0,341
5	0,290	4,383	3,339	0,531	0,887	0,423	1,615	0,232
6	0,171	6,304	2,569	0,409	0,525	0,367	1,162	0,166
7	0,456	2,239	2,639	0,420	0,554	0,615	1,042	0,327
8	0,237	4,675	2,594	0,413	0,535	0,452	1,228	0,197
9	0,265	4,453	2,594	0,413	0,535	0,424	1,392	0,163
10	0,347	3,977	3,759	0,598	1,124	0,357	1,904	0,211
11	0,376	3,378	3,329	0,530	0,882	0,477	1,613	0,261
12	0,373	3,367	3,003	0,478	0,718	0,496	1,578	0,226
13	0,631	1,992	3,738	0,595	1,112	0,621	1,580	0,437
14	0,331	3,363	2,565	0,408	0,524	0,518	1,239	0,219
15	0,267	4,813	3,434	0,547	0,938	0,426	1,651	0,242

16	0,316	4,165	3,311	0,527	0,872	0,457	1,732	0,230
17	0,274	4,646	3,141	0,500	0,785	0,352	1,621	0,170
18	0,277	4,675	3,039	0,484	0,735	0,363	1,677	0,159

Average	**0,350**	**3,792**	**3,012**	**0,479**	**0,738**	**0,481**	**1,453**	**0,244**
Median	**0,324**	**4,071**	**3,090**	**0,492**	**0,760**	**0,460**	**1,579**	**0,228**
STDEV	**0,125**	**1,172**	**0,459**	**0,073**	**0,218**	**0,102**	**0,277**	**0,081**
STDEV (%)	**36%**	**31%**	**15%**	**15%**	**30%**	**21%**	**19%**	**33%**
		Bs''				**C''**		**Rf''**
		3,426				**0,480**		**0,244**

Backlimb

Area	Drop	Channel Length	Slope	Sinuosity	Ab	W	S	R	Bl
	(m)	(km)	(m/m)	(m/m)	(km^2)	(km)	(km)		(km)
1	512	1,686	0,304	1,124	0,462	1,370	0,537	2,551	1,490
2	583	1,348	0,432	1,073	0,340	1,282	0,534	2,401	1,249
3	580	1,296	0,485	1,057	0,188	1,180	0,589	2,003	1,113
4	689	1,616	0,427	1,118	0,401	1,443	0,312	4,625	1,410
5	746	1,783	0,418	1,112	0,517	1,489	0,801	1,859	1,537
6	776	1,521	0,510	1,146	0,868	1,404	0,309	4,544	1,462
7	750	1,351	0,555	1,090	0,360	1,307	0,548	2,385	1,444
8	741	1,428	0,538	1,077	0,283	1,385	0,648	2,137	1,354
9	839	1,639	0,512	1,139	0,524	1,318	0,384	3,432	1,394
10	607	1,512	0,402	1,125	0,496	1,354	0,345	3,925	1,272
11	630	1,159	0,544	1,106	0,207	1,038	0,501	2,073	1,029
Average	**678**	**1,485**	**0,466**	**1,106**	**0,422**	**1,325**	**0,501**	**2,903**	**1,341**
Median	**689**	**1,512**	**0,485**	**1,112**	**0,401**	**1,354**	**0,534**	**2,401**	**1,394**
STDEV	**101**	**0,188**	**0,077**	**0,029**	**0,189**	**0,126**	**0,153**	**1,039**	**0,160**
STDEV (%)	**15%**	**13%**	**16%**	**3%**	**45%**	**10%**	**31%**	**36%**	**12%**
								R''	
								2,645	

Area	Bw	Bs	P	rc	Ac	C	Aq	Rf
	(km)		(km)	(km)	(km^2)		(km^2)	
1	0,400	3,725	3,858	0,614	1,184	0,390	2,220	0,208
2	0,303	4,122	2,862	0,456	0,652	0,522	1,560	0,218
3	0,252	4,417	2,777	0,442	0,614	0,306	1,239	0,152
4	0,209	6,746	3,635	0,579	1,051	0,381	1,988	0,202
5	0,531	2,895	4,547	0,724	1,645	0,314	2,362	0,219
6	0,816	1,792	4,006	0,638	1,277	0,680	2,137	0,406
7	0,325	4,443	3,544	0,564	0,999	0,360	2,085	0,173
8	0,276	4,906	3,332	0,530	0,883	0,320	1,833	0,154
9	0,406	3,433	3,646	0,580	1,058	0,495	1,943	0,270
10	0,553	2,300	3,724	0,593	1,104	0,449	1,618	0,307
11	0,281	3,662	2,480	0,395	0,489	0,423	1,059	0,195
Average	**0,396**	**3,858**	**3,492**	**0,556**	**0,996**	**0,422**	**1,822**	**0,228**
Median	**0,325**	**3,725**	**3,635**	**0,579**	**1,051**	**0,390**	**1,943**	**0,208**
STDEV	**0,178**	**1,343**	**0,597**	**0,095**	**0,330**	**0,111**	**0,412**	**0,075**
STDEV (%)	**45%**	**35%**	**17%**	**17%**	**33%**	**26%**	**23%**	**33%**
		Bs''				**C''**		**Rf''**
		3,390				**0,424**		**0,232**

Table 2: Detailed values for each measurement and parameter of each quantified drainage basin

7.3. List of Figures

1	Regional tectonics	7
2	Stratigraphic chart	10
3	Legend of the stratigraphic chart	11
4	Schematic model of fold propagation	15
5	Schematic development of merging folds	16
6	Schematic model of curved wind gaps	17
7	Development of a hogback	19
8	Measurement methods for drainage basins	20
9	Investigation area	23
10	Balanced profiles	25
11	Bana Bawi Anticline	28
12	Permam Anticline	29
13	Evolution of Permam and Bana Bawi Anticline	30
14	Evolution of Safeen Anticline	32
15	Location of the fold segments	35

8. Curriculum Vitae

Personal Details:	Name: Bernhard Bretis family status: single citizenship: Austria date of birth: 22.05.1985 place of birth: Friesach / Carinthia
Military Service:	01.09.2003 - 30.04.2004 at the signal battalion 1/Villach
Educational Details:	06/2003: high school graduation 1995 – 2003: secondary high school Feldkirchen/ Carinthia 1991 – 1995: elementary school Sirnitz/ Carinthia
University:	10/2004 – 01/2008: Bachelor studies in Earth Sciences at the University of Vienna 02/2008 – 03/2010: Master studies in Earth Sciences at the University of Vienna
Work Experience:	01.07.2003 – 31.07.2003 Internship Siemens Transportation Systems (Vienna) 01.06.2004 – 31.08.2004 Internship Siemens Transportation Systems (Vienna) 01.03.2005 – 31.09.2006 Working student Siemens AG Austria 01.08.2007 – 31.08.2007 Internship Siemens Transportation Systems (Vienna) 2009 Student tutor at the University of Vienna for “Structural Geology and Tectonics” and for “Quantification of Geological Processes”
IT- Skills:	ArcGIS, Erdas Imagine, GoCad, MathLab, River Tools, WinGeol, Windows XP, CorelDraw, MS Office, Tectonics FP

Languages: German (native speaker), English (fluent), Italian (basic)

Abstracts:

BRETIS, B., GRASEMANN, B., FABER, R. & LOCKHART, D.(2009) Fold Growth and Drainage Evolution of the Perman - Bana Bawi Anticline (Northern Iraq). *EGU General Assembly 2009*, Geophysical Research Abstracts. Vienna. 11, EGU2009-7596.

BRETIS, B., BARTL, N., GRASEMANN, B. & LOCKHART, D.(2010) Quantification of Fold Growth of Frontal Antiforms in the Zagros Fold and Thrust Belt (Kurdistan, NE Iraq). *EGU General Assembly 2010*, Geophysical Research Abstracts. Vienna.

Further Skills: blasting authority
driving licence B